OXFORD

Cerebral Cortex, 2023, **33**, 10931–10948
https://doi.org/10.1093/cercor/bhad340
Advance access publication date 18 September 2023
Original Article

Regulation of young-adult neurogenesis and neuronal differentiation by neural cell adhesion molecule 2 (NCAM2)

Alba Ortega-Gascó[1,2,†], Antoni Parcerisas[1,2,3,4,5,†], Keiko Hino[6], Vicente Herranz-Pérez[2,7,8], Fausto Ulloa[1,2], Alba Elias-Tersa[1,2], Miquel Bosch[5], José Manuel García-Verdugo[2,7], Sergi Simó[6], Lluís Pujadas[1,2,4,9,*], Eduardo Soriano[1,2,*]

[1]Department of Cell Biology, Physiology, and Immunology, Institute of Neurosciences, Universitat de Barcelona (UB), 643 Diagonal Ave., Barcelona 08028, Spain,
[2]Centro de Investigación Biomédica en Red Sobre Enfermedades Neurodegenerativas (CIBERNED), CIBER, Instituto de Salud Carlos III, 4 Sinesio Delgado, Madrid 28031, Spain,
[3]Department of Biosciences, Faculty of Sciences, Technology and Engineering, University of Vic – Central University of Catalonia (UVic-UCC), 13 Laura St., Vic 08500, Spain,
[4]Tissue Repair and Regeneration Laboratory (TR2Lab), Institut de Recerca i Innovació en Ciències de la Vida i de la Salut a la Catalunya Central (IRIS-CC), 70 Roda Rd., Vic 08500, Spain,
[5]Department of Basic Sciences, International University of Catalonia (UIC), S/N Josep Trueta St., Sant Cugat del Vallès 08195, Spain,
[6]Department of Cell Biology and Human Anatomy, University of California Davis, 1275 Med Science Dr., Davis, CA 95616, USA,
[7]Laboratory of Comparative Neurobiology, Cavanilles Institute of Biodiversity and Evolutionary Biology, University of Valencia, 7 Catedràtic Agustín Escardino Benlloch St., València 46010,Spain,
[8]Predepartamental Unit of Medicine, Faculty of Health Sciences, Jaume I University, S/N Vicent Sos Baynat Ave., Castelló de la Plana 12006, Spain,
[9]Department of Experimental Sciences and Methodology, Faculty of Heath Sciences and Wellfare, University of Vic - Central University of Catalonia (UVic-UCC), 7 Sagrada Família St., Vic 08500, Spain

*Corresponding authors: Eduardo Soriano, Department of Cell Biology, Physiology, and Immunology, Institute of Neurosciences, Universitat de Barcelona (UB), 643 Diagonal Ave., Barcelona 08028, Spain. Email: esoriano@ub.edu; Lluís Pujadas, Department of Experimental Sciences and Methodology, Faculty of Heath Sciences and Wellfare, University of Vic - Central University of Catalonia (UVic-UCC), 7 Sagrada Família St., Vic, Catalonia 08500, Spain. Email: lluis.pujadas@uvic.cat

[†]Alba Ortega-Gascó and Antoni Parcerisas contributed equally to this work.

Adult neurogenesis persists in mammals in the neurogenic zones, where newborn neurons are incorporated into preexisting circuits to preserve and improve learning and memory tasks. Relevant structural elements of the neurogenic niches include the family of cell adhesion molecules (CAMs), which participate in signal transduction and regulate the survival, division, and differentiation of radial glial progenitors (RGPs). Here we analyzed the functions of neural cell adhesion molecule 2 (NCAM2) in the regulation of RGPs in adult neurogenesis and during corticogenesis. We characterized the presence of NCAM2 across the main cell types of the neurogenic process in the dentate gyrus, revealing different levels of NCAM2 amid the progression of RGPs and the formation of neurons. We showed that *Ncam2* overexpression in adult mice arrested progenitors in an RGP-like state, affecting the normal course of young-adult neurogenesis. Furthermore, changes in *Ncam2* levels during corticogenesis led to transient migratory deficits but did not affect the survival and proliferation of RGPs, suggesting a differential role of NCAM2 in adult and embryonic stages. Our data reinforce the relevance of CAMs in the neurogenic process by revealing a significant role of *Ncam2* levels in the regulation of RGPs during young-adult neurogenesis in the hippocampus.

Key words: young-adult neurogenesis; cell adhesion molecules; corticogenesis; neuronal migration; radial glial progenitor cells.

Introduction

In mammals, active neurogenesis is preserved during adulthood by radial glial progenitors (RGPs), which remain in specific niches in the subventricular zone (SVZ) of the lateral ventricles and in the subgranular zone (SGZ) of the hippocampal dentate gyrus (DG) (Altman and Das 1965; Gonçalves et al. 2016; Gage 2019; Ghosh 2019; Kumar et al. 2019; Denoth and Jessberger 2021). Adult neurogenesis recapitulates developmental neurogenesis steps including proliferation, neuronal fate specification, migration, differentiation, synaptogenesis, and functional integration into preexistent circuits. Evidence shows that neurogenesis in the adult brain plays an important role in memory and learning processes (Zhao et al. 2008; Bergmann et al. 2015; Kumar et al. 2019). When activated, the RGPs (type I cells) produce new neurons through a process involving intermediate progenitors (type II and type III cells or neuroblasts) (Ming, and li, Song H. 2011; Kempermann et al. 2015; Gage 2019).

RGPs are located in specialized microenvironments, or neurogenic niches, where they are subjected to multiple signaling pathways that control their maintenance, proliferation, and

Received: April 29, 2022. **Revised:** August 21, 2023. **Accepted:** August 22, 2023

lineage progression (Zhao et al. 2008; Yao et al. 2016; Zhang and Zhang 2018). Cell adhesion molecules (CAMs) have been revealed as essential components of these microenvironments (Bian 2013; Morante and Porlan 2019). CAMs not only sustain the structure of the niche but also provide a link between the extracellular and the intracellular compartments of RGPs by participating in signal transduction. Different CAMs such as cadherins/protocadherins, vascular cell adhesion molecule 1, L1 cell adhesion molecule (L1CAM), and neural cell adhesion molecule 1 (NCAM1) play distinct roles in the neurogenic niches (Dihné et al. 2003; Bonfanti 2006; Angata et al. 2007; Karpowicz et al. 2009; Marthiens et al. 2010; Bian 2013; Shin et al. 2015; Boldrini et al. 2018; Morizur et al. 2018; Morante and Porlan 2019). Specifically, it has been described that CAMs could be important regulators of the quiescence/activation balance in progenitor cells (Morante and Porlan 2019). Adult RGPs are mostly found in a quiescent state, a mitotic-dormant phase in which cells display low metabolic activity but high sensitivity to signals from their environment (Urbán et al. 2019). The quiescence of RGPs is actively maintained through several mechanisms, and the regulation of the transition from quiescence to activation is crucial to preserve the pool of RGPs throughout life (Urbán and Guillemot 2014; Urbán et al. 2019).

The mammalian neural cell adhesion molecule (NCAM) family is composed of 2 members, NCAM1 and neural cell adhesion molecule 2 (NCAM2), sharing a similar structure of 5 immunoglobulin domains and 2 fibronectin type III domains, but presenting different expression patterns, posttranscriptional modifications, and molecular interactions (Pébusque et al. 1998; Makino and McLysaght 2010; Parcerisas et al. 2021a). NCAM1 is important for neuronal migration, neurite development, synaptogenesis, and it also regulates embryonic and adult neural stem cells (NSCs) during neurogenesis (Kiselyov et al. 2003; Bonfanti 2006; Angata et al. 2007; Boutin et al. 2009; Francavilla et al. 2009). NCAM2 has 2 different isoforms: NCAM2.1, a transmembrane protein with a cytoplasmatic domain, and NCAM2.2, which is glycosylphosphatidylinositol anchored (Von Campenhausen et al. 1997; Alenius and Bohm 2003). In the central nervous system, the functions of NCAM2 have been mainly linked to the regulation of axonal and dendritic formation and compartmentalization in the olfactory system (Alenius and Bohm 2003; Kulahin and Walmod 2010; Winther et al. 2012; Parcerisas et al. 2021a). It has also been related to the control of neural polarization, neurite outgrowth, dendrite development, and synapse formation and maintenance in the cortex (Cx) and hippocampus (Hp) through a complex panel of interactors (Leshchyns'Ka et al. 2015; Sheng et al. 2015; Parcerisas et al. 2020; Parcerisas et al. 2021b). *Ncam2* has been associated with different pathologies including Down Syndrome (DS), autism spectrum disorder, and Alzheimer's disease (AD). Regarding neurogenesis, *Ncam2* expression has been detected in single-cell ribonucleic acid sequencing (RNAseq) studies that characterized the genetic profiles of quiescent NSCs and their immediate progeny (Shin et al. 2015; Morizur et al. 2018). However, the role of NCAM2 in RGP biology during neurogenesis remains unknown.

In the present study, we characterized NCAM2 distribution in the young-adult hippocampal neurogenic niche and analyzed its role in the regulation of RGP biology during corticogenesis and in adulthood. To gain further insight into the importance of NCAM2 in the abovementioned processes, we used different biological and genetic approaches including in vivo hippocampal injection of viruses, in utero electroporation, and in vitro culture of NSCs. Together, our results indicate that correct NCAM2 levels are crucial for proper young-adult neurogenesis and also have a relevant role during cortical development. Moreover, our data suggest that NCAM2 participates in the fine regulation of quiescency in hippocampal RGPs, an observation that could help explain the mechanisms underlying some pathologies linked to NCAM2 such as DS, where there is an increased expression of *Ncam2*.

Materials and methods

All experimental procedures were carried out following the guidelines of the Committee for the Care of Research Animals of the University of Barcelona, in accordance with the directive of the Council of the European Community (2010/63 and 86/609/EEC) on animal experimentation. The experimental protocol was approved by the local University Committee (CEEA-UB, Comitè Ètic d'Experimentació Animal de la Universitat de Barcelona) and by the Catalan Government (Generalitat de Catalunya, Departament de Territori i Sostenibilitat).

Antibodies

The following commercial primary antibodies were used for immunohistochemistry at the indicated dilution: anti-BrdU (ab6326, Abcam; 1:500); anti-ChFP (ab167453, Abcam, 1:300); anti-DCX (A8L1U, Cell Signaling, 1:500); anti-GFP (A11122, Invitrogen, 1:2,000); anti-GFP (AB2307313, Aves Labs, 1:500); anti-GFP (ab13970, Abcam; 1:500); anti-GFAP (Z033401, DAKO, 1:2,000); anti-Ki67 (ab15580, Abcam; 1:500); anti-MAP2 (MA1406, Sigma, 1:2,000); anti-NCAM2 (AF778, R&D Systems, 1:750); anti-NCAM2.1 (EB06991, Everest, 1:500); anti-Nestin (MAB353, Chemicon, 1:100); anti-NeuN (MAB377, Merck, 1:1,000); anti-Sox2 (ab97959, Abcam, 1:500); anti-Sox2 (AF2018, R&D Systems; 1:500), and anti-Tbr2/EOMES (23,345, Abcam, 1:100). Alexa Fluor conjugated fluorescent secondary antibodies were from Invitrogen. Biotinylated secondary antibodies were from Vector Labs. Gold conjugated secondary antibodies were from UltraSmall (Electron Microscopy Sciences).

Reagents

B-27 supplement, EGF, GlutaMAX, normal horse serum (NHS), normal goat serum (NGS), penicillin/streptomycin, and trypsin were from Life Technologies. bFGF was from R&D Systems. DNaseI was from Roche diagnostic. Neurobasal medium was from Thermo Fisher Scientific. 5-Bromo-2'deoxyuridine (BrdUB52002), 2-(4-amidinophenyl)-1H-indole-6-carboxamidine (DAPI), diaminobenzidine (DAB) reagent, Durcupan ACM expoxy resin (Fluka), Eukitt, glucose, gold chloride, heparin, methylbutane, osmium tetroxide, phosphate buffer (PB), propylene oxide, sodium acetate, and Triton X-100 were from Sigma-Aldrich. Calcium chloride, hydroxide peroxide, paraformaldehyde (PFA), sodium thiosulfate, and Tris were from PanReact Applichem. Mowiol 4–48 mounting medium and sodium citrate were from Merck. Sucrose was from VWR Chemicals. Ketolar (ketamine hydrochloride 50 mg/mL) was Ritcher Pharma and Rompun (2% xylazine-thiazine hydrochloride) from Bayer. O.C.T was from Tissue-Tek. Prolong Gold anti-fade reagent was from Molecular Probes. Streptavidin-biotynilated horseradish peroxidase (HRP) was from GE Healthcare. For the electron microscopy analysis, aurion R-gent Silver enhancer kit, cold-water fish-skin gelation, and glutaraldehyde were from Electron Microscopy Sciences; bovine serum albumin-C was from Aurion.

Plasmids

To generate NCAM2.1 and NCAM2.2 overexpression vectors, the complementary deoxyribonucleic acid (cDNA) of *Ncam2.1* and *Ncam2.2* was cloned into a pWPI vector (Plasmid #12254,

Addgene) within PmeI site to obtain pWPI-NCAM2.1 and pWPI-NCAM2.2 plasmids. The cDNA of *Ncam2.1* was amplified from pCNcam2.1 with the primers 5′-ACCATGAGCCTCCTCCTCTCC-3′ and 5′-CTGACCAAGGTGCTGAAACT-3′. The cDNA of *Ncam2.2* was amplified from pCNcam2.2 with the primers 5′-ACCATGAGCCTCC TCCTCTCC-3′ and 5′-TCTCTGATCAGGGAGTACCA-3′. The pCN-CAM2.1 and pCNCAM2.2 plasmids used were previously reported in Parcerisas et al. 2020. For ShRNA vectors, ShCnt (control vector) and ShNCAM2 (NCAM2-silencing vector), constructs were obtained as described in Parcerisas et al. 2020. All vectors contain green fluorescent protein (GFP) as a reporter gene.

Production and intrahippocampal injection of lentivirus

The production and intrahippocampal injection of virus were performed as previously described (Teixeira et al. 2012; Parcerisas et al. 2020). Briefly, viral vectors were produced by transient transfection of HEK293T cells with calcium phosphate. Viral particles were concentrated by ultracentrifugation, resuspended in phosphate-buffered saline (PBS), and stored at −80°C until use. Control (pWPI), *Ncam2.1* or *Ncam2.2*-overexpressing (pWPI-Ncam2.1 or pWPI-Ncam2.2), and *Ncam2*-silencing (ShNCAM2) viruses were used to infect progenitor cells. GFP was used to identify infected cells.

For intrahippocampal injections, male wild-type C57 8-week-old mice were intraperitoneally anesthetized with a 1:10 ketamine/xylazine solution (100 μL/60 g) and placed on a heating blanket. They were positioned in a Kopf stereotaxic frame, and a midline scalp incision was made. The scalp was retracted reflected with hemostats to expose the skull, and bilateral burr holes were drilled. The coordinates used for the injections (in mm from Bregma and mm depth below the skull) were: anteroposterior −2.0, mediolateral ±1.6, and dorsoventral −2.2. Viruses were then injected (1.5 mL of viral stock solution per site) into the left and right DG over 20 min using a 5-μL Hamilton syringe. The syringe was left in place for an additional 5 min. Mice were housed in groups (2–6 mice per cage) and kept on a 12-h light–dark cycle with access to food and water ad libitum.

Histological staining and electron microscopy

Mice were anesthetized with a 10:1 mixture of ketamine/xylazine (200 μL per 60 g of weight) and intracardially perfused for 20 min with 4% PFA in 0.1 M PBS. The brains were then removed, postfixed overnight with 4% PFA in PBS, cryoprotected with 30% sucrose in PBS, and frozen. About 30 mm coronal sections of the brains were obtained with a cryostat, and immunohistofluorescence or immunohistochemistry were performed on free-floating sections. Samples were blocked with PBS containing 10% NHS, 0.3% Triton X-100, and 0.2% gelatin for 2 h at room temperature (RT); and incubated overnight at 4°C with PBS containing 5% NHS and the primary antibodies (dilutions indicated in the Antibodies section). For immunohistofluorescence, a subsequent incubation with PBS containing secondary antibodies was carried out. To counterstain nuclei, tissue and cells were incubated in DAPI (1:1,000), and the sections were mounted in Mowiol. Images were acquired with a Spectral Confocal SP2 or SP8 microscope (Leica, Wetzlar, Germany) or a Carl Zeiss LSM880 confocal microscope (Zeiss, Jena, Germany) with 10× or 60× objectives and 1,024 × 1,024 pixels resolution.

For immunohistochemistry, after the incubation with primary antibodies, a sequential incubation was carried out with biotinylated secondary antibodies and 5% NGS in PBS (2 h at RT) and then with streptavidin-biotinylated HRP complex (1:400) and 5% NGS in PBS (2 h at RT). Bound antibodies were visualized by reaction using DAB and hydrogen peroxide as peroxidase substrates, after which the sections were dehydrated and mounted in Eukitt. Images were acquired at 20× or 63× with an AF6000 microscope (Leica, Wetzlar, Germany) and an Olympus Bx61 microscope (Olympus, Shinjuku City, Tokyo, Japan).

For electron microscopy experiments, brain sections were cryoprotected in 25% sucrose and freeze-thawed (3×) in methylbutane. The sections were then washed in 0.1 M PB (pH 7.4), blocked in 0.3% bovine serum albumin-C (BSA) in PB, and incubated with a primary chicken anti-GFP antibody in blocking solution for 72 h at 4°C. The sections were washed in PB, blocked in PB containing 0.5% BSA and 0.1% cold-water fish-skin gelatin for 1 h at RT, and subsequently incubated with a colloidal gold-conjugated secondary antibody (1:50) goat anti-chicken immunoglobulin G gold in blocking solution for 24 h at RT. The sections were then washed in PB containing 2% sodium acetate. Silver enhancement was performed following the manufacturer's directions, and the sections were washed again in 2% sodium acetate in PB. To stabilize the silver particles, the samples were immersed in 0.05% gold chloride for 10 min at 4°C, washed in sodium thiosulfate, washed in PB, and then postfixed in 2% glutaraldehyde in PB for 30 min. The sections were incubated in 1% osmium tetroxide and 7% glucose in PB and then washed in deionized water. Subsequently, sections were partially dehydrated in 70% ethanol and incubated in 2% uranyl acetate in 70% ethanol in the dark for 2.5 h at 4°C. Brain slices were further dehydrated in 96% and 100% ethanol followed by propylene oxide and infiltrated overnight in Durcupan ACM epoxy resin. The following day, fresh resin was added, and the samples were cured for 72 h at 70°C. Following resin hardening, 1.5-μm semi-thin sections were selected under light microscopy based on their immunolabeling and detached from the glass slides by repeatedly freezing and thawing in liquid nitrogen. Ultrathin sections (60–70 nm) were obtained from selected semi-thin sections. Photomicrographs were obtained using a FEI Tecnai G^2 Spirit transmission electron microscope (FEI Europe, Eindhoven, Netherlands) using a Morada digital camera (Olympus Soft Image Solutions GmbH, Münster, Germany).

In utero electroporation

In utero microinjection and electroporation were performed at embryonic day (E) 14.5 as previously described (Simó et al. 2010; Parcerisas et al. 2020), using timed pregnant CD-1 mice (Charles River Laboratories). Briefly, deoxyribonucleic acid (DNA) solutions were mixed in 10 mM Tris (pH 8.0) with 0.01% Fast Green. Needles for injection were pulled from Wiretrol II glass capillaries (Drummond Scientific) and calibrated for 1-μL injections. Forceps-type electrodes (Nepagene) with 5-mm pads were used for electroporation (5 50-ms pulses of 45 V at E14.5). Brains were collected at either E19.5-postnatal day (P) 0 or at P5, dissected, and those with successful electroporations were identified by epifluorescence microscopy. GFP- or cherry fluorescent protein (ChFP)-positive brains were fixed in 4% formalin in PBS and cryoprotected with 30% sucrose in PBS overnight at 4°C. Brains were frozen in O.C.T compound before 14-μm-thick brain cross-sections were obtained with cryostat and placed on slides. Sections were antigen-retrieved by immersion of the slides in 0.01 M sodium citrate buffer, pH 6.0 at 95°C for 20 min. Sections were blocked with 10% NGS, 10 mM glycine, and 0.3% Triton X-100 in PBS for 2 h at RT. Primary antibodies (anti-GFP and anti-ChFP) were incubated overnight at 4°C. Slides were washed 4 times for 10 min in 0.1% Triton X-100 in PBS. Secondary antibodies were added for 2 h at RT, and the slides were washed as before and

coverslipped with Prolong Gold anti-fade reagent. Images were obtained with epifluorescent illumination and a 10× objective with Leica760 (Leica, Wetzlar, Germany) and AF6000 microscopes (Leica, Wetzlar, Germany). Data were collected from the lateral part of the anterior neocortex. For quantification of neurons in bin10, the Cx was divided into bins as follows: the distance from the bottom of the SVZ to the pial surface was measured and divided into 10 equally sized bins. The position of GFP- or ChFP-positive neurons was analyzed in 3–5 sections per embryo. The percentage of GFP- or ChFP-labeled neurons in each bin relative to the total number of GFP- or ChFP-labeled neurons across the 10 bins was then calculated for each section.

NSC culture

NSCs were isolated from the Hp of 7–8 postnatal day (P7–P8) mice following the modified protocol described by Walker and Kempermann 2014. Briefly, the Hp was dissected in PBS. After trypsin and DNaseI treatments, the tissue was dissociated with a gentle sweeping motion. Cells were counted and cultured as neurospheres or adherent monolayers in Neurobasal medium containing 2% B-27 supplement, 100 U/mL penicillin/streptomycin and 1X GlutaMAX, 20 ng/mL epidermal growth factor (EGF), 20 ng/mL basic fibroblast growth factor (bFGF), and 2 mg/mL heparin. Cells were incubated at 37°C with a 5% CO_2 atmosphere and subcultured every 2–3 days.

Neurosphere growth analysis

For the analysis of neurosphere growth, SGZ-derived neurospheres were dissociated with trypsin and infected at passage 2 with lentiviruses containing either pWPI, pWPI-NCAM2.1, pWPI-NCAM2.2, ShNCAM2, or ShCnt. Successfully infected, GFP-positive cells were selected by flow cytometry (BD FACSAria Fusion, San Jose, California, USA), plated in nonadherent 24-well plates, and the resulting neurospheres analyzed during 5 consecutive days. High-content image acquisition was performed with an automated wide-field Olympus IX81 microscope (Olympus Life Science Europe, Waltham, MA) and an UPlan FL N 4× objective. ScanR Acquisition Software version 2.3.0.5 was used to automatically image 20 adjacent fields per well (5 × 4 grid) acquiring a z-stack for each field (8 z-planes with a z-step of 200 nm). A 10% overlap was set to enable automatic image stitching. Neurosphere area was obtained with a set of 3 custom-made macros in Fiji to project each z-stack, stitch these projections, and calculate the area of each neurosphere. The frequency distribution according to their area was analyzed for the different conditions (Control, NCAM2.1 or NCAM2.2-overexpressing and NCAM2-silencing).

BrdU proliferation assay

NSCs isolated from the Hp of 7–8 postnatal day (P7–P8) mice were counted and plated in coverslips treated with poly-D-lysine (10 μg/mL, Sigma) and laminin (5 μg/mL, Sigma). Cells were infected with viruses (pWPI, pWPI-NCAM2.1, pWPI-NCAM2.2, ShCnt, and ShNCAM2) and maintained in neurobasal medium containing 2% B-27 supplement, 100 U/mL penicillin/streptomycin and 1X GlutaMAX, 20 ng/mL EGF, 20 ng/mL bFGF, and 2 μg/mL heparin. After 3 days of infection, cells were incubated with 10 μM BrdU during 4 h at 37°C. Treated cells were fixed in 4% PFA for 15 min at RT. For the detection of BrdU, DNA hydrolysis was performed prior to the immunostaining. Samples were sequentially incubated with HCl 1 M and 1 M borate buffer. After permeabilization with PBS 0.1% Triton X-100 for 5 min, cell cultures were blocked with 10% NHS and incubated in 5% serum with anti-GFP and anti-BrdU primary antibodies for 2 h at RT. Cells were incubated with secondary antibodies (Alexa Fluor, Invitrogen) and DAPI and finally mounted (Mowiol, Calbiochem). Images were acquired with Leica Thunder DMi8 (Leica) and Carl Zeiss LSM880 (Zeiss) microscopes at 20×, 25×, and 40× with a resolution of 1,024 × 1,024. The results are presented as the ratio of change of NCAM2-silenced cultures compared to controls.

NSCs differentiation

For the analysis of NSCs differentiation, neurospheres were dissociated at passage 3 and plated in adherent coverslips treated with poly-D-lysine (10 mg/mL) and laminin (5 mg/mL). Cells were infected with control (pWPI or ShCnt), NCAM2.1 and NCAM2.2-overexpressing (pWPI-NCAM2.1, pWPI-NCAM2.2), and NCAM2-silencing (ShNCAM2) viruses and maintained in neurobasal medium containing 2% B27 supplement, penicillin/streptomycin, and GlutaMAX, without growth factors, at 37°C and 5% CO_2 for 5 days. The differentiated cultures were fixed in 4% PFA for 15 min at RT.

Cell cultures were permeabilized with PBS 0.1% Triton X-100 for 5 min, blocked with 10% NHS, and incubated in 5% serum with anti-GFP and anti-MAP2 primary antibodies for 2 h at RT. Cells were incubated with secondary antibodies (Alexa Fluor, Invitrogen) and DAPI and finally mounted (Mowiol, Calbiochem). Images were acquired by epifluorescence (Olympus Bx61, Olympus and Leica Thunder DMi8, Leica) and confocal microscopes (Carl Zeiss LSM880, Zeiss) microscopy at 20×, 25×, and 40× with a resolution of 1,024 × 1,024.

Statistical analysis

Statistical analysis was carried out using GraphPad Prism 8 software (San Diego, CA, USA). For the characterization of the cells infected with GFP-encoding lentiviruses, we calculate the percentage of GFP/Sox2/glial fibrillary acidic protein (GFAP) triple positive and GFP/doublecortin (DCX) or GFP/neuronal nuclei double positive cells. Additionally, we quantified the proportion of Ki67-positive cells among the GFP/Sry-related HMG box transcription factor (Sox2)/GFAP population. For the GFP/Sox2/GFAP triple positive condition, data were also normalized for a better comparison by considering as 100% the values found for the first time point (3d). To determine differences between groups in the adult neurogenesis characterization experiments, one-way analysis of variance (ANOVA) was used. Post hoc comparisons were performed by Tukey's test. Statistical significance between groups in distribution of cells during corticogenesis was assessed by 2-way ANOVA followed by Bonferroni's post hoc comparison test. For the analysis of NSCs in vitro, differences between control and overexpressing conditions were assessed by one-way ANOVA with post hoc comparisons performed by Tukey's or Kruskal–Wallis test. To determine differences between control and NCAM2-silenced cultures, we used a t-Student test.

Results

Differential expression pattern of NCAM2 in the DG

Since CAMs are important structural elements of the neurogenic niches, we first characterized the distribution of NCAM2 in the different cell populations of the DG of P45 mice by immunofluorescence. DG RGPs express different markers while undergoing several morphological and electrophysiological changes through the neurogenic process that finally gives rise to mature neurons. We used GFAP/Sox2 (double labeling) or Nestin as markers to identify type I progenitors, while T-box brain protein 2 was selected to

label type II proliferative progenitors (Kempermann et al. 2015). In addition, we detected type III progenitors (neuroblasts) or immature neurons with antibodies against DCX, and mature neurons with NeuN labeling.

As NCAM2 is a membrane protein, the overall pattern of NCAM2 staining clearly delineated the cell bodies and dendrites of neurons. Confocal microscopy analysis revealed strong NCAM2 signal in GFAP/Sox2-positive cells and in Nestin-positive cells with the typical morphology of type I progenitors (i.e. triangular cell bodies located in the SGZ and a single apical process extending into the molecular layer) (Fig. 1A and B; Supplementary Fig. 1A and B). Contrariwise, images suggested lower levels of NCAM2 levels in Tbr2-positive cells, although it is difficult to determine the presence of both NCAM2 and Tbr2 in the same cell due to the different localization of each protein (NCAM2 is a membrane-bound protein while Tbr2 is a nuclear factor) (Fig. 1C; Supplementary Fig. 1C). Among the DCX-positive cell population, we found several phenotypes with differences in NCAM2 staining. Although some DCX-positive cells displayed faint or undetectable NCAM2 signal, other cells presented higher levels of the protein (Supplementary Figs. 2A and 3A). Lastly, mature granule cells (GCs) that expressed NeuN also presented NCAM2 labeling, as expected (Supplementary Figs. 2B and 3B).

Therefore, the distribution pattern of NCAM2 in the DG of the Hp suggests a differential expression across the neurogenic lineage: Although both type I progenitors (RGPs) and mature neurons present noticeable NCAM2 staining, the intermediate type II–III progenitors may have decreased NCAM2 levels.

NCAM2 modulates adult neurogenesis in the DG

To study the potential role of NCAM2 in adult neurogenesis, we modulated the levels of NCAM2 protein in the hippocampal neurogenic region. We stereotaxically injected the DG of 8-week-old mice with GFP-containing *Ncam2.1*-overexpressing (pWPI-NCAM2.1), *Ncam2.2*-overexpressing (pWPI-NCAM2.2), *Ncam2*-silencing (ShNCAM2), or control lentiviruses (pWPI or ShCnt), which bear preferential infectivity on progenitor cells and neuroblasts (Consiglio et al. 2004; Jandial et al. 2008). We analyzed the transduced DGs 4 weeks after surgery. Mice injected with control viruses exhibited infected cells with a characteristic morphology of dentate GCs (i.e. round soma in the granular layer, and apical dendrites ramifying in the molecular layer and covered with dendritic spines) (Fig. 2A, top left panel). Similar results were found in mice injected with *Ncam2*-silencing viruses, indicating that the downregulation of *Ncam2* does not substantially alter the formation or maturation of adult-born neurons in the DG. (Fig. 2A, top right panel). Conversely, we found that many cells infected with either *Ncam2.1*- or *Ncam2.2*-overexpressing viruses did not exhibit the typical morphology of maturing GCs but an RGP-like phenotype (i.e. triangular cell bodies located in the inner granule layer (GL) with a single, short radial process spanning the GL and ramifying profusely in the inner molecular layer) (Fig. 2A, bottom panels). Some of the cells infected with the overexpression viruses, however, resembled type II progenitors or neuroblasts (i.e. cells with an irregular soma and short processes oriented tangentially, or with a rounded soma and a short apical dendrite oriented toward the molecular layer) or immature GCs. Enrichment in cells with a RGP-like phenotype was apparently more prominent upon *Ncam2.2* than *Ncam2.1* overexpression.

To further characterize the phenotype of *Ncam2*-overexpressing cells, we performed an ultrastructural analysis of the infected cells by GFP immunogold staining and electron microscopy imaging (Fig. 2B). Confirming the above results, most control virus-infected cells at the injection site corresponded to dentate GCs which were densely arranged in the GL (Fig. 2B). These cells showed a typical round soma, most of it occupied by the nucleus, which displayed chromatin aggregates. The cytoplasm comprised a thin space with few long cisternae of endoplasmic reticulum and abundant free ribosomes. Nevertheless, we also observed a few control virus-infected cells in the SGZ that resembled RGPs and type II progenitors and neuroblasts (Fig. 2B). In contrast, *Ncam2.1*- and *Ncam2.2*-overexpressing cells were detected mainly in the SGZ (Fig. 2B). These GFP-labeled cells in the SGZ exhibited a large cell body with a major radial process that penetrated the GL and extended thin lateral processes among granule neurons. They presented round or triangular nucleus, irregular contour, and intermediate filaments in their electron-lucent cytoplasm (Fig. 2B). These ultrastructural features are characteristic of RGPs (Seri et al. 2004). On the other hand, type II cells and neuroblasts were also identified among *Ncam2.1*- and *Ncam2.2*-overexpressing cells that exhibited a smooth contour, dark and scant cytoplasm, abundant polyribosomes, and a less well-developed endoplasmic reticulum than that of GCs (Fig. 2B). These results support that *Ncam2* overexpression could lead to an arrest of infected cells in an RGP/type II progenitor state.

Cell-autonomous overexpression of *Ncam2* retains adult-born DG cells in an RGP-like phenotype

To better understand the sequence of events triggered by the expression of *Ncam2* isoforms, mice injected with control and *Ncam2*-overexpressing viruses were sacrificed at different time points: 3 days, 1 week, 2 weeks, and 4 weeks postinjection (Fig. 3A). Although the infection was not strictly restricted to progenitor cells, as expected, the majority of the infected cells in all the experimental conditions exhibited an RGP morphology at 3 days postinjection (Consiglio et al. 2004; Jandial et al. 2008) (Fig. 3B, Supplementary Fig. 4). When analyzing later time points, most cells infected with control viruses showed a morphology typical of immature GCs at 1 week post-injection, which progressed toward a more mature morphology by 2- and 4 weeks postinjection. In contrast, the morphology of *Ncam2.1*- or *Ncam2.2*-overexpressing cells remained constant over time, with most of the infected cells exhibiting an RGP-like cell morphology, while others showed intermediate progenitor- or neuroblast-like phenotypes (Fig. 3B).

The phenotype of cells infected with the viral vectors was additionally characterized by evaluating the expression of specific cell markers at the different time points analyzed. A GFP/Sox2/GFAP triple immunostaining was used to determine the proportion of RGPs within the pool of infected (GFP-positive) cells (Fig. 4A and B). At 3 days postinjection, most infected cells in all experimental conditions were GFP/Sox2/GFAP-triple positive (Supplementary Fig. 4). When analyzing the progression of GFP/Sox2/GFAP-triple positive progenitors in the control condition, we observed a statistically significant, progressive reduction in the number of progenitors over time (Fig. 4C and D). In contrast, in the animals infected with *Ncam2.1*- or *Ncam2.2*-overexpressing viruses, we noticed a much less marked decrease in the proportion of those progenitors over time, thus suggesting an arrest of the cells in the progenitor stage (Fig. 4C and D). In contrast, in the animals infected with *Ncam2.1*- or *Ncam2.2*-overexpressing viruses, we noticed a much less marked decrease in the proportion of those progenitors over time, thus suggesting an arrest of the cells in the progenitor stage (Fig. 4C and D).

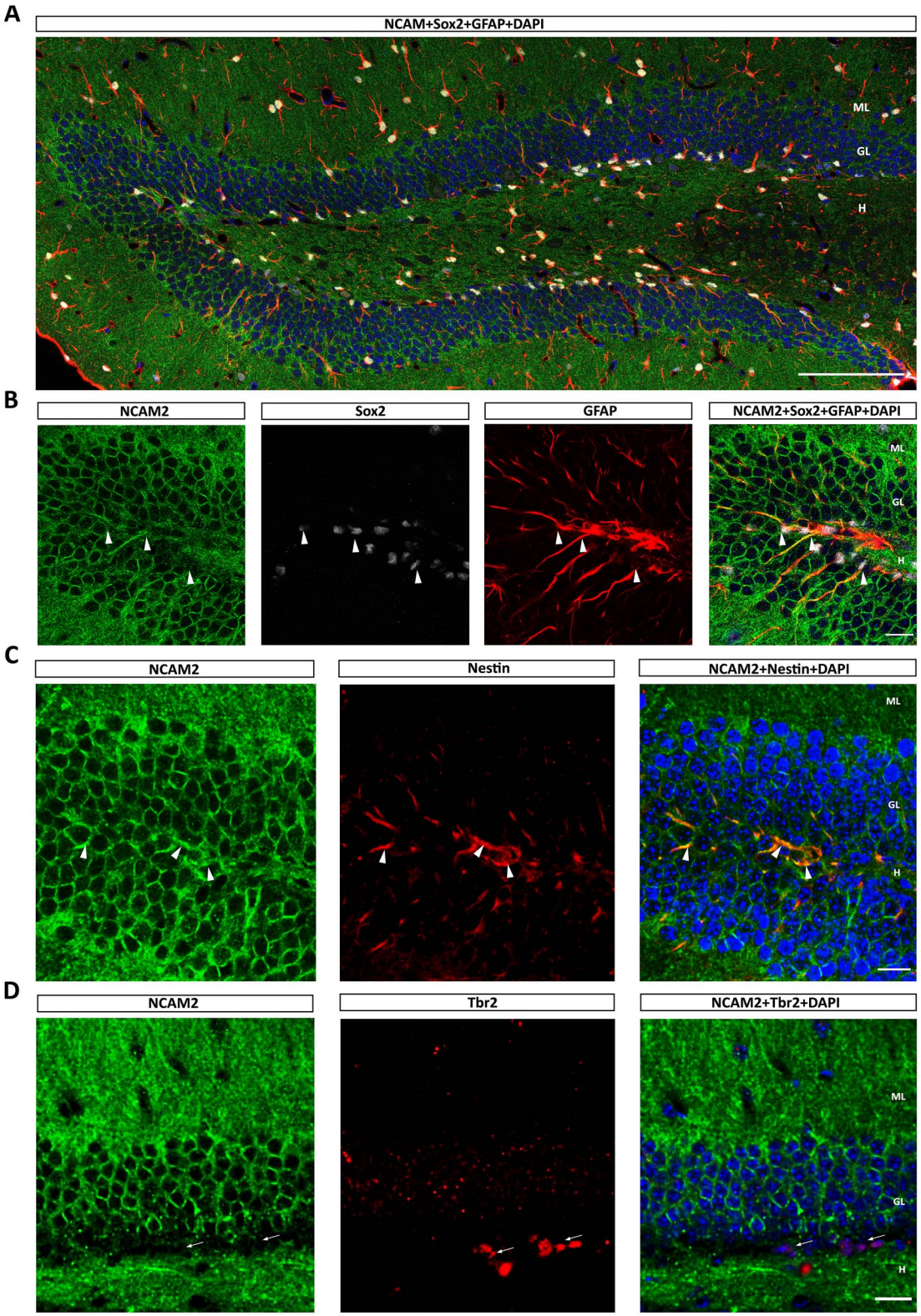

Fig. 1. Distribution of NCAM2 in the hippocampal progenitor cells. A and B) Immunohistochemical characterization of NCAM2 distribution in Sox2/GFAP-positive progenitor cells in P45 mouse DG. Arrowheads indicate NCAM2/Sox2/GFAP triple positive cells with anti-NCAM2.1 antibody (Everest, EB06991) B). C) NCAM2 immunostaining in nestin-positive cells in the SGZ of P45 mouse brain. Arrowheads indicate NCAM2/nestin-positive cells. D) Double immunostaining of NCAM2 and Tbr2 at P45. Arrows indicate Tbr2-positive cells that present low NCAM2 signal. ML: molecular layer; GL: granule layer; H: hilus. Scale bars: A) 50 μm, B), C) 20 μm.

We confirmed that most *Ncam*2.1- and *Ncam*2.2-overexpressing cells morphologically characterized as neuronal progenitor cells did express the neuronal progenitor markers GFAP and Sox2 at 1 week post-injection (Fig. 4A and C). Additionally, quantifications revealed a maintenance of high proportion of GFP/Sox2/GFAP-triple positive cells at 2 weeks and 4 weeks in both *Ncam*2.1 and *Ncam*2.2 overexpression groups, with a more pronounced effect in the case of the *Ncam*2.2 isoform (Fig. 4B–D).

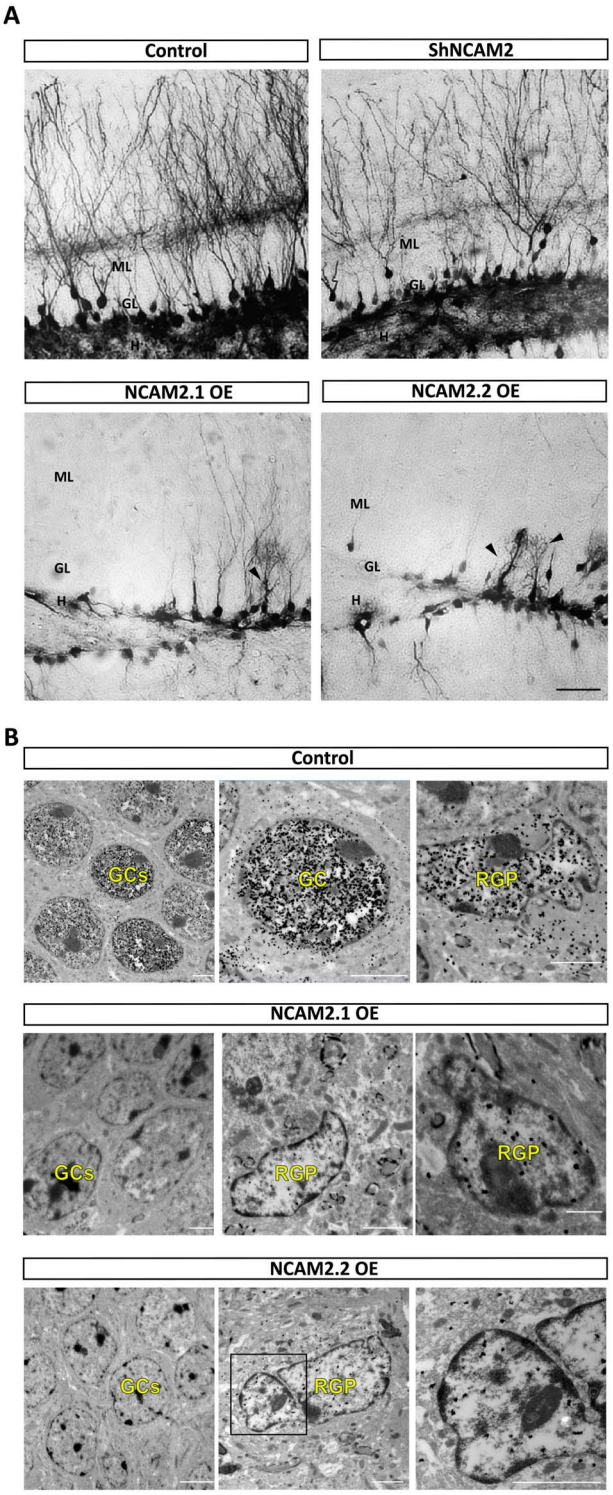

Fig. 2. *Ncam2* overexpression modulates adult neurogenesis in the Hp. A) Representative images of GFP-positive cells in the DG of mice injected with control, ShNCAM2, or *Ncam2*-overexpressing viruses (*Ncam2.1* or *Ncam2.2*) 4 weeks after injection. Control and ShNCAM2-infected cells showed a GC morphology, while an RGP-like phenotype was observed in many cells infected with *Ncam2.1*- or *Ncam2.2*-overexpressing viruses. B) GFP immunogold electron microscopy images of mice infected with control, *Ncam2.1*-, or *Ncam2.2*-overexpressing viruses and sacrificed 4 weeks postsurgery. Control condition images show densely GFP-labeled GCs and RGPs (NSCs). In *Ncam2.1*- and *Ncam2.2*-overexpressing conditions, the number of labeled GCs was dramatically decreased. Nevertheless, GFP-labeled RGPs located in the SGZ were still noticeable. ML: molecular layer; GL: granule layer; H: hilus; GC: granule cell; RGP: radial glial progenitor; OE: overexpressing. Scale bars: A) 50 μm, B) 2 μm.

The analysis of the impact of *Ncam2* overexpression in neurogenesis was complemented by quantifying the number of DCX-positive cells at 2- and 4 weeks post-injection (Fig. 5A). According to the expected progression of neurogenic events, in the control condition, we observed a marked reduction in the percentage of DCX-positive cells between weeks 2 and 4 postinjection (Fig. 5C). Such decline was not detected when either *Ncam2.1* or *Ncam2.2* were overexpressed, in which case we found a persisting number of DCX-positive cells from 2 to 4 weeks postinjection. Finally, the number of NeuN-positive, mature neurons at 4 weeks post-injection was also analyzed (Fig. 5B). In agreement with the results presented above, we found a trend toward reduced percentages of NeuN-positive neurons in the *Ncam2* overexpression conditions at 4 weeks post-injection, which reached statistical significance in the *Ncam2.2* isoform compared to controls (Fig. 5D).

This time-course analysis suggests that the observations at 4 weeks post-injection in *Ncam2* overexpression conditions are not attributable to a dedifferentiation of immature neurons into progenitor-like cells, but rather to a temporary arrest of SGZ cells in an RGP-like phenotype that leads to a delay in the formation of new neurons.

The overexpression of NCAM2 decreases RGPs proliferation

To determine the proliferative capacity of the infected progenitor cells, we evaluated the expression of the Ki67 marker in the GFP/Sox2/GFAP-positive cell population in animals sacrificed at 3 days and 4 weeks postinjection (Fig. 6A and B). As anticipated, no statistically significant differences were observed in the percentage of Ki67-positive progenitors between control and *Ncam2.1*- or *Ncam2.2*-overexpressing groups at 3 days after injection (Fig. 6C). However, at 4 weeks after injection, the overexpression of NCAM2 resulted in lower percentages of Ki67+ cells among the GFP/Sox2/GFAP-positive cells (Fig. 6D). This reduction was significant when the isoform NCAM2.2 was upregulated (Fig. 6D). These findings suggest that the overexpression of NCAM2 has an inhibitory effect on the proliferation of NSC progenitors.

Ncam2 overexpression does not arrest embryonic RGPs in neurogenic areas

Since our results point out to an important role of NCAM2 in the regulation of adult RGPs and because NCAM1 is involved in both adult and embryonic neurogenesis (Angata et al. 2007; Boutin et al. 2009), we next sought to study the potential role of NCAM2 during embryonic cortical development. We performed in utero electroporation experiments using isoform-specific overexpressing vectors that contained GFP or ChFP as reporter genes. Embryos were electroporated at E14.5, coinciding with the onset of NCAM2 expression, and brains were analyzed at P0 and P5. In the neocortex, the progression of RGPs into subsequent cell types during the neurogenic process is paralleled by their migration to upper layers. Therefore, to understand whether progenitors were arrested at any point, we evaluated the distribution of electroporated E15-born neurons across cortical layers. Interestingly, at P0, we found a nonsignificant increase of cells located in neurogenic areas (subventricular zone and intermediate zone) in cortices electroporated with the 2 *Ncam2* isoforms alone or in combination (Fig. 7A). In addition, we observed alterations in the migration of neurons when modulating *Ncam2* expression (Fig. 7A). Our

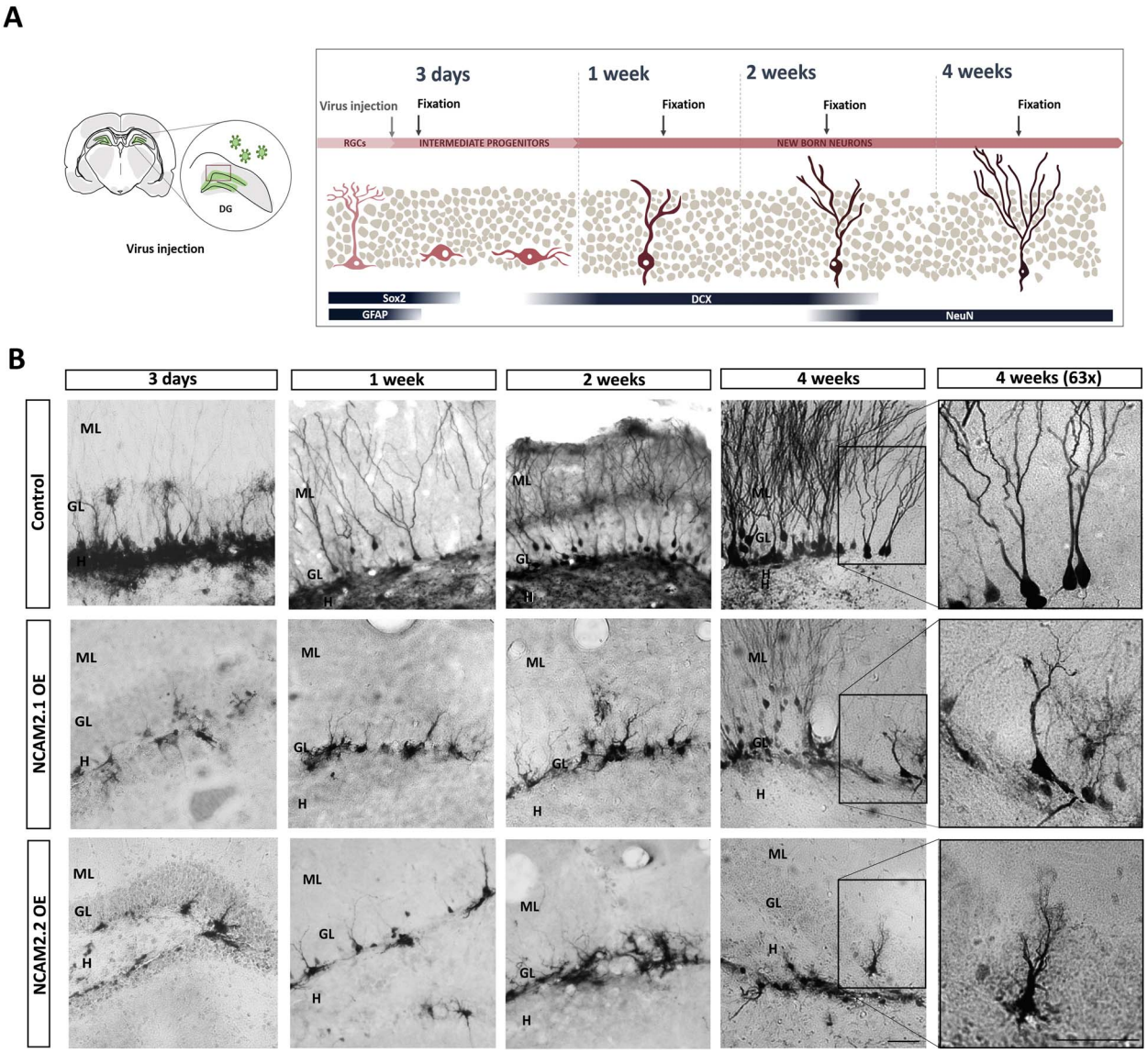

Fig. 3. Time-course analysis of the NCAM2 effect on adult neurogenesis. A) Schematic representation of the experimental approach in parallel with the adult hippocampal neurogenesis process. Eight-week-old mice were injected in the DG area with control, *Ncam2.1*,- or *Ncam2.2*-overexpressing lentiviruses with GFP as a reporter gene, and sacrificed at the indicated time points after surgery. B) Exemplary images of the DG at 3 days, 1 week, 2 weeks, and 4 weeks after injection of control or *Ncam2*-overexpressing viruses. Higher magnification images of representative cells revealed the presence of infected cells with an RGP-like morphology in the animals injected with *Ncam2*-overexpressing viruses. ML: molecular layer; GL: granule layer; H: hilus; OE: overexpressing. Scale bar: 50 μm.

previous study (Parcerisas et al. 2020) showed that both *Ncam2* isoforms are expressed in the developing Cx, and that their expression is necessary for correct neuronal migration, since *Ncam2* knockdown leads to neuronal mispositioning. In the present analysis, at P0, most E15-born control neurons were located in the upper portion of the cortical plate (CP) and displayed a typical immature pyramidal neuron shape, with a main apical dendrite directed toward the marginal zone (MZ) (Fig. 7A and B).

In the case of E15-born *Ncam2.2*-overexpressing neurons, we observed an altered distribution with a significant reduction of neurons in the uppermost portion of the CP (bin 10) compared with the control condition (Fig. 7A and B). E15-born *Ncam2.1*-overexpressing neurons showed a tendency to also be located below bin 10 as compared with control neurons (Fig. 7A–C). A synergistic effect was found when embryos were electroporated with both isoforms (*Ncam2.1* + *Ncam2.2*) simultaneously (Fig. 7A and B). In addition, and in contrast with *Ncam2* depletion (Parcerisas et al. 2020), *Ncam2* overexpression apparently does not disrupt normal dendritic arborization at P0 (Fig. 7E).

Conversely, at P5, E15-born neurons displayed a similar distribution in control and *Ncam2*-overexpressing conditions, with most neurons being located in the lower part of layers II–III (Fig. 7C and D). Overall, we found that *Ncam2.1* and *Ncam2.2* overexpression, alone or in combination, did not result in an arrest of cortical progenitor cells in the VZ at any of the stages analyzed. Our results suggest that, in contrast to the situation in the adult Hp, *Ncam2.1* and *Ncam2.2* overexpression in cortical progenitors leads to transient migratory deficits, but not to their arrest in progenitor-like phenotypes in the VZ.

NCAM2 overexpression impairs NSCs differentiation in vitro

The implications of NCAM2 in young-adult neurogenesis were further investigated in vitro. We first analyzed the proliferation

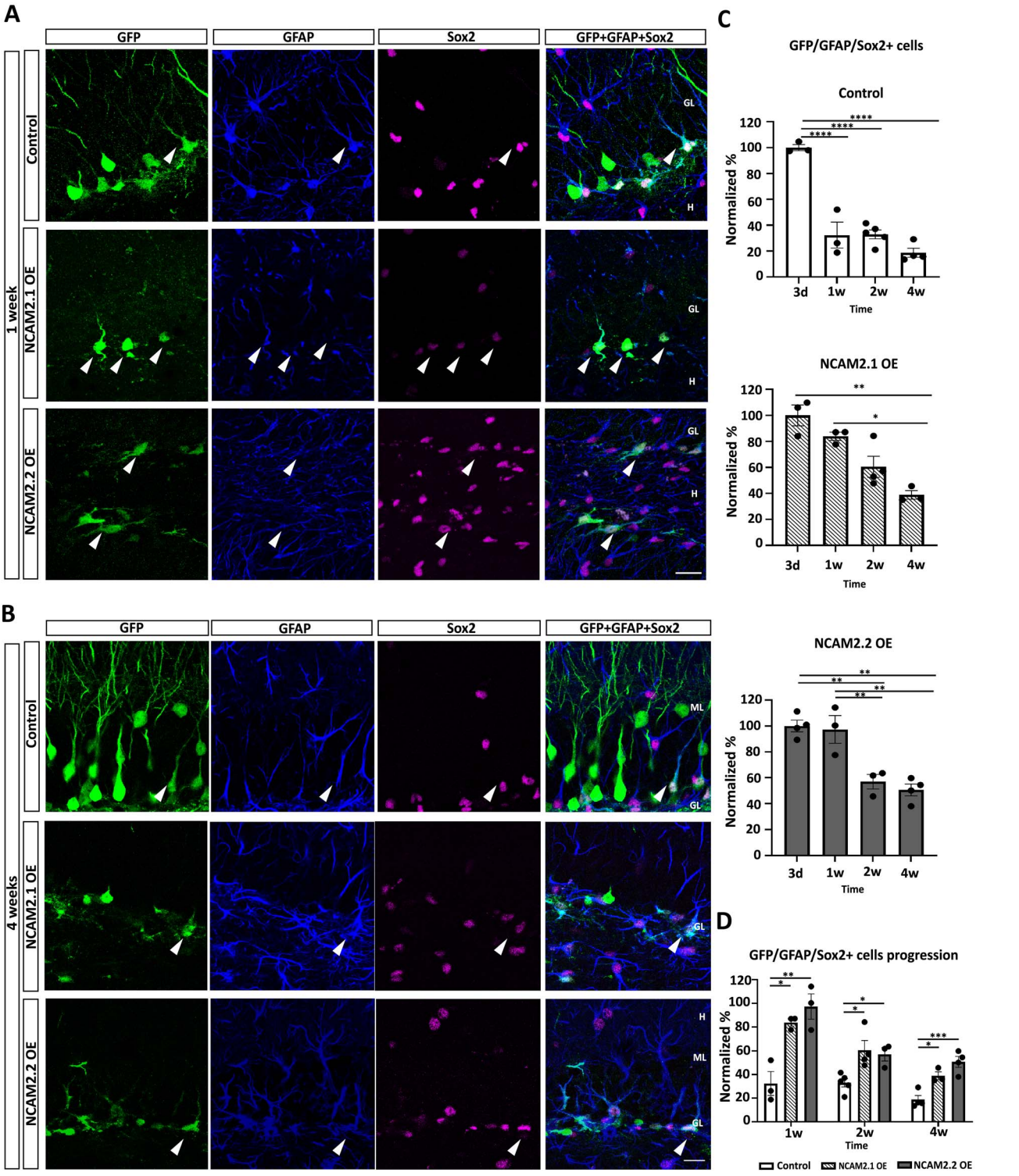

Fig. 4. Immunohistochemical characterization of *Ncam2*-overexpressing progenitor cells. A) Immunostaining with GFP (marker for infected cells) and the RGP markers GFAP and Sox2 hippocampal sections of mice sacrificed 1 week after injection of control or *Ncam2.1*- or *Ncam2.2*-overexpressing lentiviruses. B) Same immunostaining and lentivirus conditions as in A) in mice sacrificed at 4 weeks postinjection. C–D) Time-course quantification of the normalized percentage of GFP/Sox2/GFAP-positive cells in mice injected with control, *Ncam2.1*-, or *Ncam2.2*-overexpressing viruses at 3 days, 1 week, 2 weeks, and 4 weeks post-injection. $N = 3–5$ animals per group, 5–10 sections per animal, 20–50 cells per animal. Data are presented as mean ± SEM; dots represent mean values for individual animals; ANOVA, Tukey's comparison post hoc test; $^{*}P < 0.05$, $^{**}P < 0.01$, $^{***}P < 0.001$, $^{****}P < 0.0001$. Arrowheads label GFP/Sox2/GFAP-positive cells. ML: molecular layer; GL: granule layer; H: hilus; OE: overexpressing; d, day; w, week. Scale bars: A, B) 20 μm.

of NSCs grown as neurospheres and infected with control, ShNCAM2, *Ncam2.1-overexpressing*, or *Ncam2.2*-overexpressing viruses (Supplementary Fig. 5). As NCAM2 is a CAM, it is challenging to discern whether the effects on the area of the neurospheres are due to altered proliferative rates or changes in cell adhesion. To overcome these limitations, we analyzed the proliferation of NSCs in adherent cultures derived from the Hp of P6–7 mice. Cells were infected with control or ShNCAM2 co-expressing GFP as a reporter

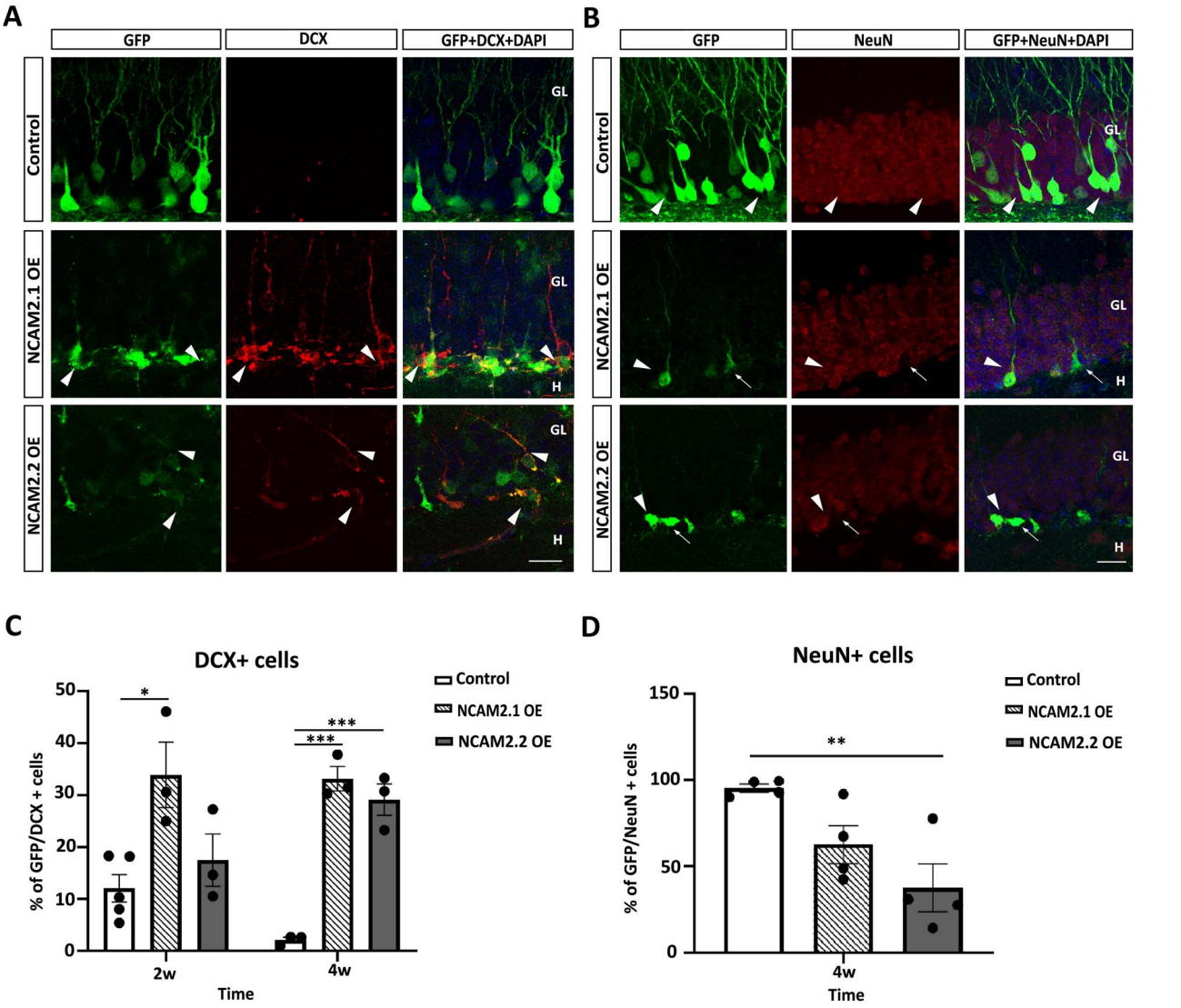

Fig. 5. Immunohistochemical characterization of *Ncam2*-overexpressing neurons. A) Immunostaining with GFP (marker for infected cells) and DCX as a marker for neuroblasts (type III progenitors) and immature neurons in DG sections of mice sacrificed 4 weeks after injection of control or *Ncam2.1*- or *Ncam2.2*-overexpressing lentiviruses. B) Immunostaining with GFP (marker for infected cells) and NeuN as marker for mature neurons in DG sections of the same mice and conditions as in A). C) Quantification of the percentage of GFP/DCX-positive cells in mice injected with control, *Ncam2.1*-, or *Ncam2.2*-overexpressing viruses at 2 weeks and 4 weeks post-injection. $N = 3$–4 animals per group, 5–6 sections per animal (>50 cells per animal in the control and 15–30 cells per animal in the *Ncam2*-overexpressing conditions). D) Quantification of the percentage of GFP/NeuN-positive cells in animals injected with control, *Ncam2.1*-, or *Ncam2.2*-overexpressing viruses at 4 weeks postinjection. $N = 4$ animals per group, 5 sections per animal (>50 cells per animal). Data are presented as mean ± SEM; dots represent mean values for individual animals; differences between experimental groups: ANOVA, Tukey's comparison post hoc test; $^{*}P < 0.05$, $^{**}P < 0.01$, $^{***}P < 0.001$. Arrowheads indicate DCX- or NeuN-positive, GFP-positive cells; arrows indicate NeuN-negative, GFP-positive cells. GL: granule layer; H: hilus; OE: overexpressing; w, week. Scale bars: A, B) 20 μm.

gene. When cells reached confluency, we assessed their proliferative capacity using a BrdU incorporation assay. The analysis of BrdU/GPF positive cells showed an increased percentage of BrdU-positive cells when the expression of NCAM2 is downregulated (Supplementary Fig. 6). Those findings suggest that NCAM2 could regulate the proliferation of NSCs in vitro.

The above in vivo and in vitro studies indicate that NCAM2 expression arrests infected progenitors into a RGP phenotype and reduces proliferation. To evaluate the effects of NCAM2 in neuronal differentiation, NSC grown as neurospheres was dissociated and plated in PDL/laminin coated plates after passage 3. Cells were infected with control, *Ncam2*-overexpressing, or *Ncam2*-silencing viruses and cultured in adherent conditions for 3 days before removal of the bFGF and EGF growth factors. Cultures were then maintained for 5 additional days to allow cell differentiation (Fig. 8A). Interestingly, we observed GFP/microtubule-associated protein 2 (MAP2)-positive cells in the *Ncam2*-overexpressing conditions (Fig. 8B), indicating that NCAM2 does not totally block the differentiation of progenitor cells to neurons. However, quantitative analyses revealed a lower percentage of GFP/MAP2 cells in SGZ NCAM2.1- and NCAM2.2-overexpressing cells, compared to controls (Fig. 8C). We did not detect differences in the number of MAP2 positive cells when NCAM2 was silenced (Supplementary Fig. 6D and E).

The in vitro data reinforce the in vivo evidences suggesting a contribution of NCAM2 in regulation of young-adult neurogenesis. Together, the results presented here suggest that fine regulation of NCAM2 expression levels is relevant, with overexpression leading

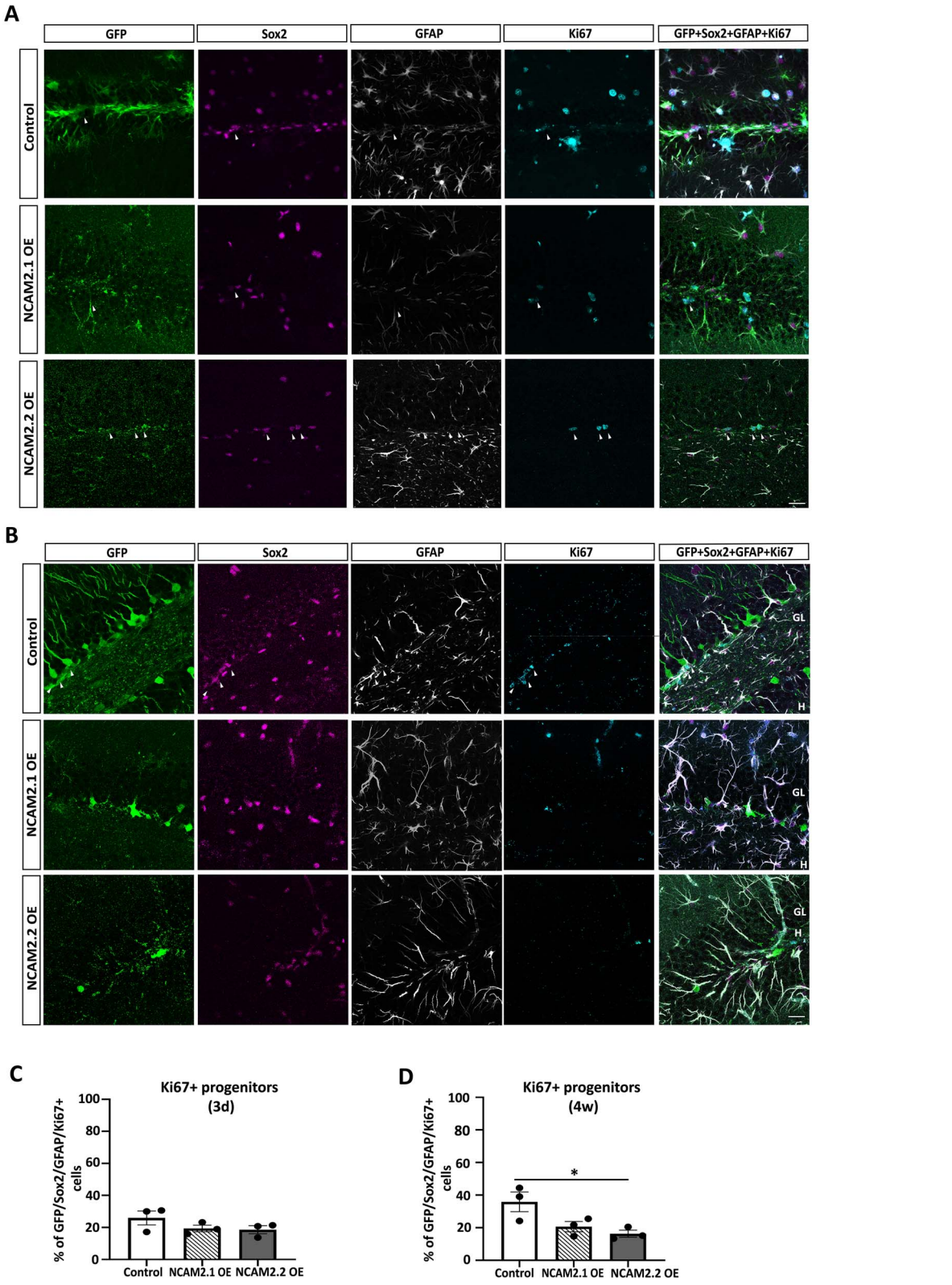

Fig. 6. Analysis of Ki67 expression in the GFP/Sox2/GFAP positive cells. A) Immunostaining with GFP, GFAP, and Sox2 and the proliferative marker Ki67 in hippocampal sections of mice sacrificed 3 days after injection of control or *Ncam2.1*- or *Ncam2.2*-overexpressing lentiviruses. B) Immunostaining with GFP/GFAP/Sox2 and Ki67 in samples of mice sacrificed at 4 weeks postinjection. C) Percentage of Ki67-positive cells among the GFP/Sox2/GFAP progenitor population in mice injected with control, *Ncam2.1*-, or *Ncam2.2*-overexpressing viruses at 3 days postinjection. N = 3 animals per group, 5–10 sections per animal, 20–50 cells per animal. D) Quantifications of Ki67-positive cells among the GFP/Sox2/GFAP progenitors in mice injected with control, *Ncam2.1*-, or *Ncam2.2*-overexpressing viruses at 4 weeks postinjection. N = 3 animals per group, 5–10 sections per animal, 20–50 cells per animal. Data are presented as mean ± SEM; dots represent mean values for individual animals; ANOVA, Tukey's comparison post hoc test; $^*P < 0.05$. Arrowheads label GFP/Sox2/GFAP/Ki67-positive cells. ML: molecular layer; GL: granule layer; H: hilus; OE: overexpressing; d, day; w, week. Scale bars: A, B) 20 μm.

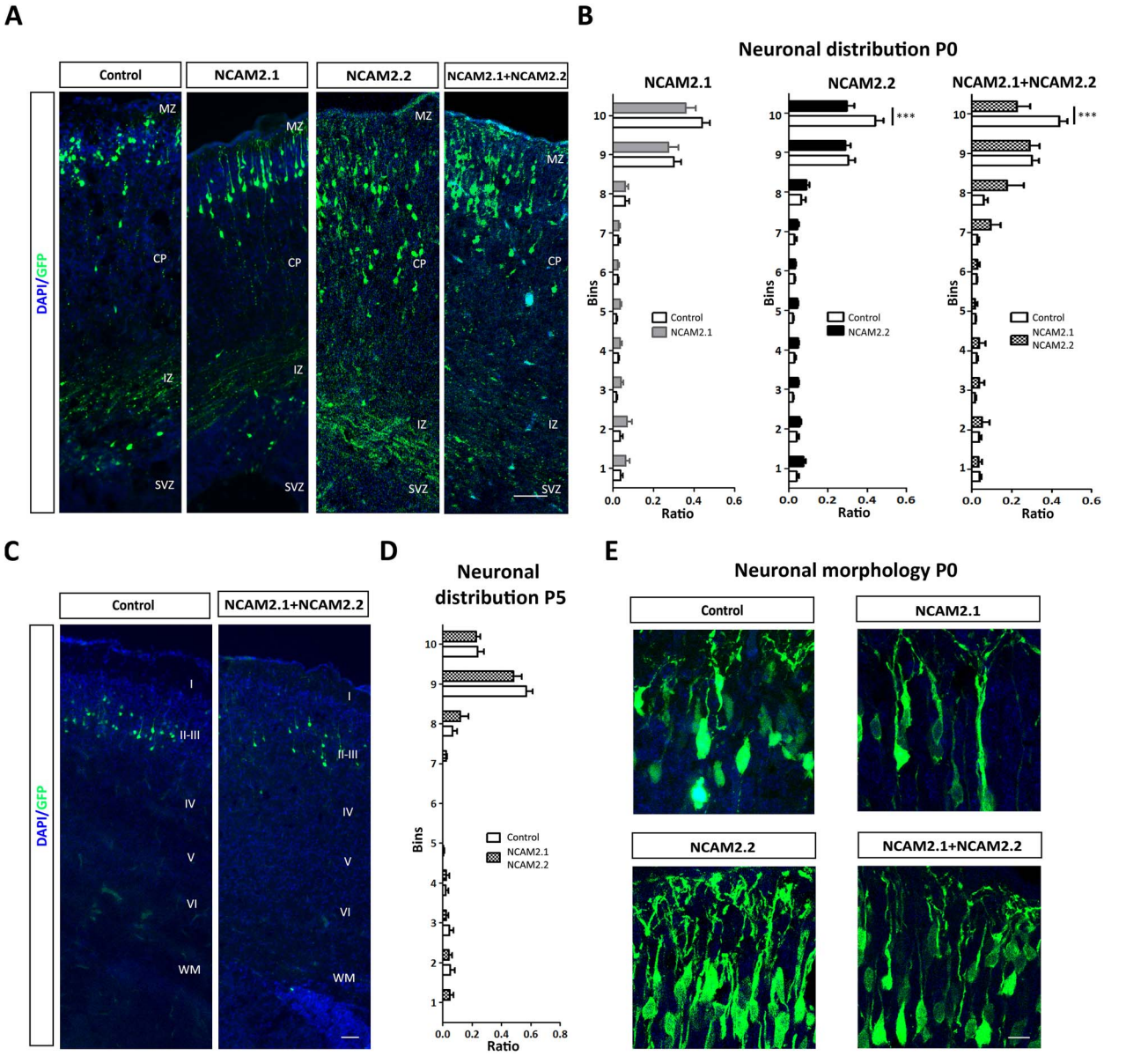

Fig. 7. *Ncam2* overexpression does not arrest embryonic RGPs but affects neuronal migration. A) Representative images of E15-born GFP-positive electroporated neurons in cortical sections from P0 mice. Neurons were electroporated with control or *Ncam2* overexpression vectors alone or in combination. B) The distribution of transfected cells across cortical layers at P0 was analyzed by dividing the distance from the SVZ to the pial surface in 10 bins. Data are presented as the ratio of electroporated neurons with somas located in each bin. Overexpression of *Ncam2.2* and simultaneous overexpression of both isoforms (*Ncam2.1* + *Ncam2.2*) induced a reduced proportion of cells in the uppermost bin. $N = 5$–8 animals electroporated with control or overexpression constructs, 3–4 sections per animal; $^{***}P < 0.001$; 2-way ANOVA with Bonferroni comparison post hoc test. C) Representative images of E15-born GFP-positive electroporated neurons in cortical sections from P5 mice. Neurons were electroporated with control or a combination of overexpression vectors for both isoforms (*Ncam2.1* + *Ncam2.2*). D) The distribution of transfected cells across cortical layers was analyzed at P5 in 10 bins, and data are presented as in B). No differences in neuronal distribution were found between control and NCAM2-overexpressing conditions at P5. $N = 6$ animals electroporated with the constructs, 3–4 sections per animal; 2-way ANOVA with Bonferroni comparison post hoc test. E) Higher magnification of representative images of transfected neurons at P0. Neurons showed normal pyramidal neuronal morphology. CP, cortical plate; IZ, intermediate zone; MZ, marginal zone; SVZ, subventricular zone; I–VI, cortical layers I–VI; WM, white matter. Scale bars: A, D) 50 μm; E) 10 μm.

to retention of progenitor cells in undifferentiated stages. Transitory depletion of NCAM2 expression could favor proliferation and differentiation of young-adult progenitors into maturing neurons.

Discussion

The present work provides a deeper understanding on the functions of NCAM2 during young-adult neurogenesis and embryonic development in mice. Our results indicate that NCAM2 levels regulate the RGP-to-immature neuron transition in the adult DG. In contrast, our data suggest that physiological levels of NCAM2 are not crucial for cortical neurogenesis, but transiently relevant for cortical migration.

Neurogenic niches are necessary for the regulation of adult RGP properties, as they convey the different physiological stimuli that induce the activation of quiescent radial glial progenitors (qRGPs) and regulate their division, survival, and differentiation. Recently, CAMs have been revealed as important elements in the cytoarchitecture and signaling of the neurogenic reservoirs (Kokovay et al. 2012; Bian 2013; Porlan et al. 2014; Morizur et al. 2018). In the present study, we characterized the distribution of NCAM2 molecule in the hippocampal SGZ niche. By

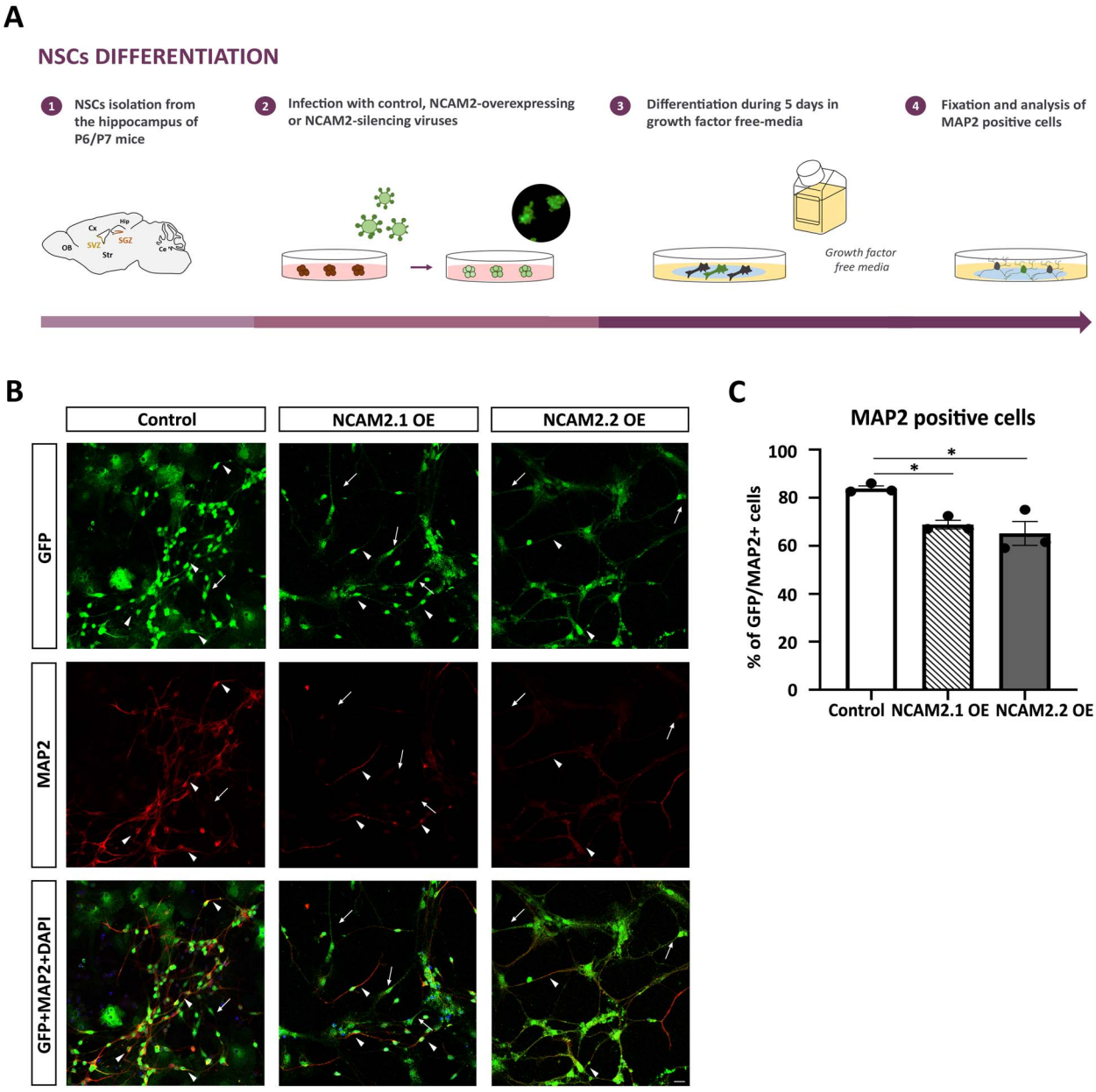

Fig. 8. Effect of NCAM2 expression in NSCs differentiation. A) Scheme showing the protocol for the obtention of postnatal mouse NSCs from the neurogenic niches. Isolated cells were grown as neurospheres, infected with control, *Ncam2*-overexpressing, or *Ncam2* silencing viruses; and dissociated after 3 passages. Neurospheres were dissociated, plated in adherent coverslips, and maintained 5 days in differentiation conditions before fixation. B) Representative images of differentiated cultures infected with control, *Ncam2*.1-, or *Ncam2*.2-overexpressing viruses after 5 days upon differentiation conditions immunostained with MAP2 neuronal marker. Arrows indicate GFP/MAP2 double labeled cells. Arrowheads indicate GFP-positive cells not labeled with MAP2. C) Quantification of GFP/MAP2-positive cells in control or *Ncam2*-overexpressing cell cultures. Data presented as mean ± SEM; one-way ANOVA, Tukey's comparison post hoc test, $^*P < 0.05$. Scale bar: 20 μm.

immunodetecting NCAM2 in the SGZ populations, we revealed differential levels of the protein among the main actors in the neurogenic process. The observed pattern of NCAM2 suggests high *Ncam2* expression in type I progenitors and low levels in intermediate progenitors, although alternative methods would be necessary to corroborate the downregulation of *Ncam2* in those transient amplifying progenitors (Fig. 9). Once the proliferative stage is completed, the levels of NCAM2 seem to undergo a progressive increase in the newborn DCX-positive, maturing neurons until reaching high levels in NeuN-positive neurons as NCAM2 becomes necessary to participate in dendrite development, axon formation, and synaptogenesis (Alenius and Bohm 2003; Kulahin and Walmod 2010; Winther et al. 2012; Parcerisas et al. 2020) (Fig. 9). The NCAM2 distribution pattern is supported by previous single-cell RNA data (Shin et al. 2015; Morizur et al. 2018). The genetic profiles of RGPs and their progeny show an enrichment in *Ncam2* in qRGPs, and a decrease in *Ncam2* levels during the activation of RGPs and their transition to intermediate progenitors (Supplementary Fig. 7) (Codega et al. 2014; Shin et al. 2015; Morizur et al. 2018; Xie et al. 2020).

Our data show how changes in NCAM2 levels modify the normal course of the neurogenic events. The infection of progenitor cells from hippocampal SGZ with *Ncam2*-overexpressing lentiviruses seems to arrest these cells in an RGP-like phenotype and delay the formation of new GCs, as we characterized by morphological, immunohistochemical, and ultrastructural

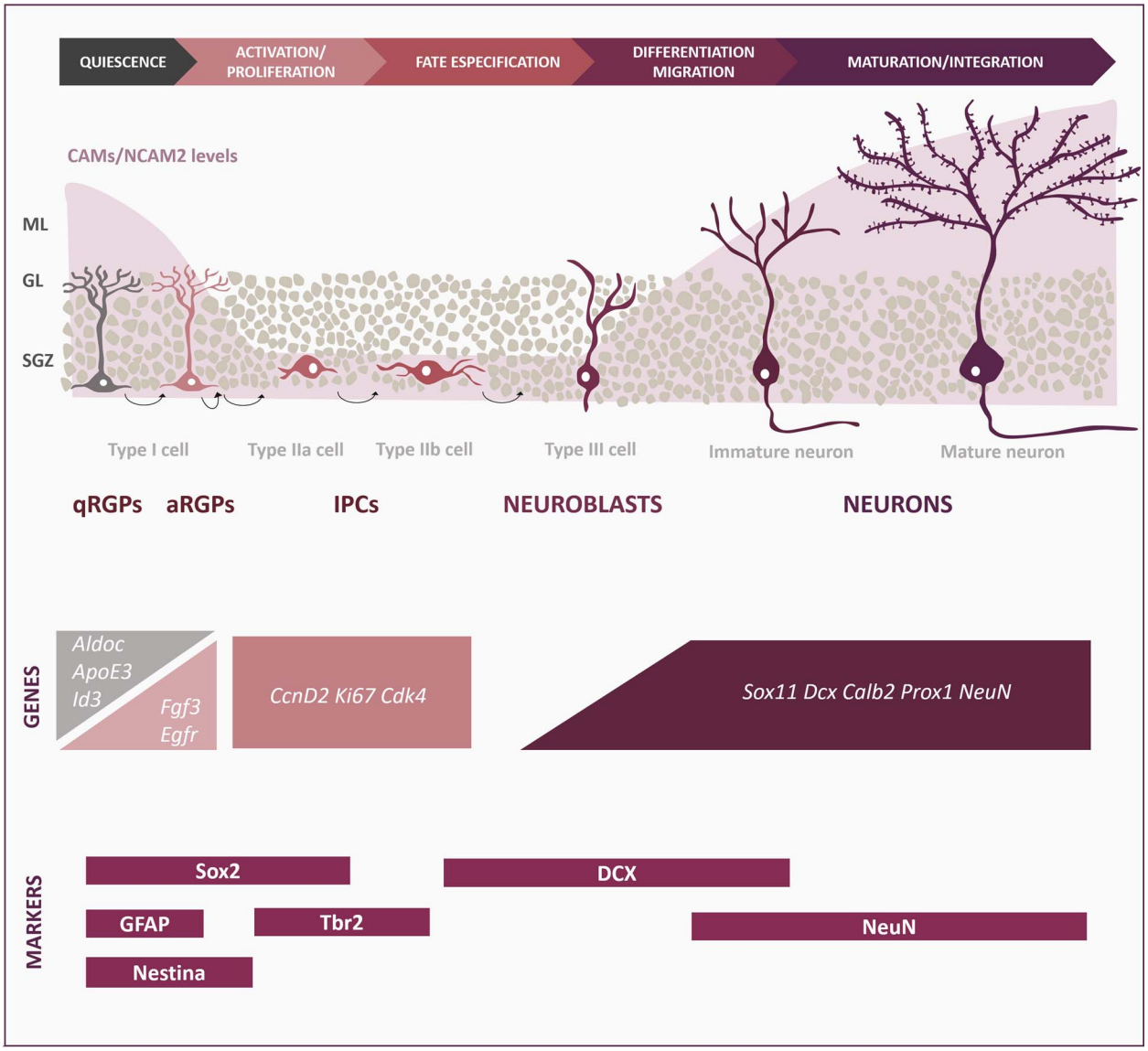

Fig. 9. Model of RGP regulation by *Ncam2* expression levels in the Hp. Schematic representation of the proposed model for NSC regulation by *Ncam2* expression. RGPs (type I cells) are GFAP/Sox2/nestin positive and are maintained in a quiescent state in the SGZ of the DG. Upon activation, RGPs generate Tbr2-positive proliferating intermediate progenitors (type II cells). In turn, these transit-amplifying progenitors produce neuroblasts (type III cells) that express DCX and differentiate into NeuN-positive GCs. Newborn neurons mature and become functional neurons of the hippocampal circuits through a process regulated by different intrinsic and extrinsic factors. We postulate that the levels of CAMs such as NCAM2 protein are crucial for the regulation of RGPs quiescence, the activation of their proliferation, and for the proper neuronal differentiation and maturation in later stages (Shin et al. 2015; Morizur et al. 2018; Parcerisas et al. 2020). aRGP, activated radial glial progenitor; IPC: Intermediate progenitor cell, qRGP, quiescent radial glial progenitor.

analyses. Despite using VSV g pseudotyped lentivirus that preferentially infect progenitor cells for the gene transduction (Consiglio et al. 2004; Jandial et al. 2008), the resulting infection was not strictly restricted to progenitor cells, specially in the control conditions. The different number of cells infected by control and overexpressing viruses could be explained by the increased vector size of the NCAM2-overexpressing plasmids that affect vector production and transduction efficiency (Kumar M et al., 2001; Canté-Barrett et al., 2016; Sweeney & Vink, 2021). For this reason, we analyzed differences in percentages and not in total number of infected cells. Regardless of the variations in the transduction efficiency, the majority of the infected cells at the starting point are progenitors in all the conditions, and the impact of NCAM2 overexpression on the modulation of young-adult neurogenesis is clear. Conversely, inducing *Ncam2* depletion in this hippocampal neurogenic zone did not lead to an increase in the number of newly produced neurons. The underlying cause for this inconsistency might lie on the technical limitations that hinders from infecting a uniform and comparable number of cells across conditions, hence precluding a quantitative analysis of the total population of newborn neurons.

To overcome these limitations, we further investigated the effect of NCAM2 in vitro using a BrdU incorporation assay in NSCs adherent cultures. We observed that *Ncam2* downregulation in progenitor cells in vitro significantly increases the proliferation of NSCs. The effects of NCAM2 in the proliferation of NSCs in vitro have been previously observed in progenitor cells that form the spinal cord (Deleyrolle et al. 2015), which supports the data obtained in the present study.

Diverse underlying mechanisms could explain the effects of *Ncam2* overexpression in the neurogenic process. The upregulation of NCAM2 levels could affect the survival of the newborn

cells, induce the dedifferentiation of developing neurons, or alter the differentiation of the newborn neurons. However, considering the distribution pattern of NCAM2 and the time-course analysis of the events (Codega et al. 2014; Morizur et al. 2018; Xie et al. 2020), we propose that a fine regulation of *Ncam2* expression levels would be necessary for maintaining RGP quiescence and activating their proliferation. Previous data show the relevance of CAMs in the regulation of stem cell quiescence/activation balance (Codega et al. 2014; Porlan et al. 2014; Shin et al. 2015; Morizur et al. 2018; Xie et al. 2020). Our interpretation is that high levels of NCAM2 may arrest cells in a quiescent state, while the downregulation of *Ncam2* may allow RGPs to exit quiescence and enter the cell cycle to proliferate and differentiate (Fig. 9).

A temporary retention of cells in the progenitor stages would lead to a delay in the cascade of neurogenic events, leading to increased percentages of DCX immature neurons at 2 and 4 weeks postinjection, and thus postponing the generation and maturation of GCs 4 weeks after infection. Nonetheless, other explanations may also contribute to the phenotype observed (e.g. changes in cell survival or differentiation to other cell types). Further research is needed to understand the molecular mechanisms by which NCAM2 regulates RGP quiescence, cell proliferation, and differentiation in adulthood. However, one hypothesis is that NCAM2 could interact with growth factor receptors such as the epidermal growth factor receptor (EGFR) or the fibroblast growth factor receptor (FGFR). Growth factors are important regulators of the activation and proliferation of qRGPs (Aguirre et al. 2010; Urbán et al. 2019); and it has been described that FGFR and EGFR receptors interact with NCAM2, as well as with others CAMs (L1CAM or NCAM1) (Kulahin et al. 2008; Francavilla et al. 2009; Deleyrolle et al. 2015; Rasmussen et al. 2018). Another possibility is that NCAM2 expression could cause cytoskeletal rearrangements, which are known to influence the neurogenic process (Kronenberg et al. 2010; Parcerisas et al. 2020; Parcerisas et al. 2021b).

Interestingly, the effect of *Ncam2* overexpression in the regulation of adult RGPs was not observed in embryonic cortical progenitors. When modulating the expression of *Ncam2* in embryonic RGPs, we did not find a retention of progenitor cells in the VZ but a transiently altered neuronal distribution, suggesting a delay in the migration of progenitors during cortical development. In spite of the embryonic origin of adult RGPs, adult and embryonic progenitors are subject to a distinct regulation (Urbán and Guillemot 2014; Berg et al. 2018; Daniel Berg et al. 2019). Although embryonic RGPs have a high proliferative rate, necessary for the rapid growth of neural tissues (Urbán and Guillemot 2014; Urbán et al. 2019), adult RGPs are mostly found in a quiescent state to avoid the exhaustion of the stem cell pool (Urbán et al. 2019). Therefore, the functions of NCAM2 in regulating stem cell quiescence seem to be more critic during adulthood than in development. In contrast, NCAM2 seems to be necessary for the regulation of cortical migration. Our previous results also showed that the downregulation of *Ncam2* leads to an alteration of cortical migration, which results in mislocalization of layer II–III-fated neurons and altered morphology (Parcerisas et al. 2020). Neuronal migration is a key process in corticogenesis, the disruption of which is associated to many diseases including autism spectrum disorder and schizophrenia (Hussman et al. 2011; Petit et al. 2015; Scholz et al. 2016). The mechanisms underlying the effects of NCAM2 on neuronal migration are not known. However, an interaction has been described between NCAM2 and microtubule-associated proteins, which also participate in the regulation of neuronal migration (González-Billault et al. 2005; Kawauchi and Hoshino 2008; Parcerisas et al. 2020; Parcerisas et al. 2021a).

The functional relevance of NCAM2-dependent regulation of hippocampal neurogenesis is still to be explored. Modulation of neurogenesis by running or exposure to enriched environment would be of great interest to be studied in animal models with up- or downregulation of the gene to assess the impact of NCAM2 on learning abilities. Moreover, in light of all this evidence, NCAM2 could be related to the neurogenic deficits described in some murine models of pathologies such as AD, schizophrenia, or epilepsy. In particular, the trisomy of chromosome 21, which causes DS, leads to a gene-dosage effect that results in an increased expression of *Ncam2* gene (Kahlem et al. 2004; Palmer et al. 2021). Our data correlate with the neurogenic alterations proposed in DS mouse models that display a reduced proliferation of progenitor cells and a lower number of differentiated neurons (Lorenzi and Reeves 2006; Hewitt et al. 2010; Belichenko and Kleschevnikov 2011; López-Hidalgo et al. 2016). In the present study, we show that the overexpression of *Ncam2* produces an arrest of the cells in an RGP state and a reduction in newly formed neurons, suggesting a correlation with the neurogenic deficits described in DS mouse models.

Neurogenic niches are complex microenvironments where RGPs receive and interact with multiple signals. CAMs are key elements for the transduction of the signals and the regulation of stem cell behavior. Our work provides evidence for a remarkable function of NCAM2 in the regulation of RGPs during young-adult neurogenesis. Furthermore, we reveal the importance of *Ncam2* expression in regulating neuronal migration and differentiation during corticogenesis in the embryonic development. Overall, the present study contributes to a better understanding of the implications of NCAM2 during neuronal development and adult plasticity, and opens new research lines to explore the molecular basis of DS pathogenesis.

Acknowledgments

We thank A. Lladó and S. Tosi (microscopy facility of the IRB-Barcelona) for FIJI macro design and technical assistance in ScanR acquisition; *L. Badia* (microscopy facility of the IRB-Barcelona) for support and technical assistance; E. Coll and M. Calvo (microscopy facilities of the University of Barcelona) for technical assistance; M. Pérez (Universitat Internacional de Catalunya) for technical support in viral production; the members of the Department of Cell Biology, Physiology and Immunology (University of Barcelona), in particular J. Correas for cryostat support and E. Verdaguer for valuable support; and members of the Soriano lab for experimental help and comments.

Authors' contributions

E.S., L.P., A.O-G., and A.P. conceived and designed the study. A.O-G. and A.P. performed most of the experiments and analyzed data. K.H. and S.S. designed and performed the in utero electroporation experiments. V.H-P. and J.M.G-V. designed, conducted, and analyzed the electron microscopy experiments. F.U. supervised the characterization of RGPs. A.E-T and M.B participated in some experiments. A.O-G., A.P., V.H.-P., L.P., and E.S. wrote the manuscript. All authors read and revised the manuscript.

CRediT authors' contributions

Alba Ortega-Gascó (Conceptualization, Data curation, Formal analysis, Investigation, Methodology, Writing—original draft,

Writing—review & editing), Antoni Parcerisas (Conceptualization, Data curation, Formal analysis, Investigation, Methodology, Writing—original draft, Writing—review & editing), Keiko Hino (Methodology, Writing—review & editing), Vicente Herranz-Pérez (Investigation, Methodology, Resources, Visualization, Writing—review & editing), Fausto Ulloa (Methodology, Supervision), Alba Elias-Tersa (Methodology, Writing—review & editing), Miquel Bosch (Methodology, Resources, Writing—review & editing), Jose Manuel Garcia-Verdugo (Methodology, Resources, Writing—review & editing), Sergi Simó (Methodology, Resources, Supervision, Writing—review & editing), Lluís Pujadas (Conceptualization, Data curation, Funding acquisition, Supervision, Validation, Writing—original draft, Writing—review & editing), and Eduardo Soriano (Conceptualization, Data curation, Funding acquisition, Project administration, Resources, Supervision, Validation, Writing—original draft, Writing—review & editing).

Supplementary material

Supplementary material is available at *Cerebral Cortex* online.

Funding

This work was supported by grants from the Spanish Ministry of Science, Innovation and Universities to V.H-P. (PCI2018-093062), to M.B. (PID2020-118817GB-I00), to E.S. and L.P. (PID2019-106764RB-C21/ AEI/ 10.13039/501100011033 and Excellence Unit 629, María de Maeztu/Institute of Neurosciences) and to A.O.-G. (BES-2017-080570).; from the Spanish Ministry of health (ISCIII-CIBERNED) and from the Secretariat of Universities and Research of the Department of Economy and Knowledge of the Generalitat de Catalunya to A.P.; from the Valencian Council for Innovation, Universities, Science and Digital Society (PROMETEO/2019/075) to J.M.G-V.; and from the National Institute of Health (NIH) (R01NS109176) to S.S.

Conflict of interest statement: None declared.

Data availability

The data that supports the findings of this study are available from the corresponding author upon reasonable request.

References

Aguirre A, Rubio ME, Gallo V. Notch and EGFR pathway interaction regulates neuralstem cell number and self-renewal. *Nature*. 2010:467:323–327.

Alenius M, Bohm S. Differential function of RNCAM isoforms in precise target selection of olfactory sensory neurons. *Development*. 2003:130:917–927.

Altman J, Das GD. Post-natal origin of microneurones in the rat brain. *Nature*. 1965:207:953–956.

Angata K, Huckaby V, Ranscht B, Terskikh A, Marth JD, Fukuda M. Polysialic acid-directed migration and differentiation of neural precursors are essential for mouse brain development. *Mol Cell Biol*. 2007:27:6659–6668.

Belichenko PV, & Kleschevnikov AM. Deficiency of Adult Neurogenesis in the Ts65Dn Mouse Model of Down Syndrome. In Dey S, editor. *Genetics and Etiology of Down Syndrome*. London: InTech; 2011. p. 177–192.

Berg DA, Bond AM, Ming G, Song H. Radial glial cells in the adult dentate gyrus: what are they and where do they come from. *F1000Research*. 2018:7:1–12.

Bergmann O, Spalding KL, Frisén J. Adult neurogenesis in humans. *Cold Spring Harb Perspect Med*. 2015:5(7):1–12.

Bian S. Cell adhesion molecules in neural stem cell and stem cell-based therapy for neural disorders. In Bonfanti L, editor. *Neural stem cells – new perspectives*. London: InTech; 2013. p.349–380.

Boldrini M, Fulmore CA, Tartt AN, Simeon LR, Pavlova I, Poposka V, Rosoklija GB, Stankov A, Arango V, Dwork AJ, et al. Human hippocampal neurogenesis persists throughout aging. *Cell Stem Cell*. 2018:22:589–599.

Bonfanti L. PSA-NCAM in mammalian structural plasticity and neurogenesis. *Prog Neurobiol*. 2006:80(3):129–164.

Boutin C, Schmitz B, Cremer H, Diestel S. NCAM expression induces neurogenesis in vivo. *Eur J Neurosci*. 2009:30:1209–1218.

Canté-Barrett K., Mendes R. D., Smits W. K., van Helsdingen-van Wijk Y. M., Pieters R. & Meijerink, *J. P. Lentiviral gene transfer into human and murine hematopoietic stem cells: size matters. BMC research notes*. 2016:9:1–6.

Codega P, Silva-Vargas V, Paul A, Maldonado-Soto AR, DeLeo AM, Pastrana E, Doetsch F. Prospective identification and purification of quiescent adult neural stem cells from their in vivo niche. *Neuron*. 2014:82:545–559.

Consiglio A, Gritti A, Dolcetta D, Follenzi A, Bordignon C, Gage FH, Vescovi AL, Naldini L. Robust in vivo gene transfer into adult mammalian neural stem cells by lentiviral vectors. *Proc Natl Acad Sci U S A*. 2004:101:14835–14840.

Daniel Berg AA, Su Y, Jimenez-Cyrus D, Ming G-L, Song H, Bond Correspondence AM, Berg DA, Patel A, Huang N, Morizet D, et al. A common embryonic origin of stem cells drives developmental and adult neurogenesis article a common embryonic origin of stem cells drives developmental and adult neurogenesis. *Cell*. 2019:177:654–668.

Deleyrolle L, Sabourin JC, Rothhut B, Fujita H, Guichet PO, Teigell M, Ripoll C, Chauvet N, Perrin F, Mamaeva D, et al. OCAM regulates embryonic spinal cord stem cell proliferation by modulating ErbB2 receptor. *PLoS One*. 2015:10:e0122337.

Denoth-Lippuner A, Jessberger S. Formation and integration of new neurons in the adult hippocampus. *Nat Rev Neurosci*. 2021:22(4):1–14.

Dihné M, Bernreuther C, Sibbe M, Paulus W, Schachner M. A new role for the cell adhesion molecule L1 in neural precursor cell proliferation, differentiation, and transmitter-specific subtype generation. *J Neurosci*. 2003:23:6638–6650.

Francavilla C, Cattaneo P, Berezin V, Bock E, Ami D, De Marco A, Christofori G, Cavallaro U. The binding of NCAM to FGFR1 induces a specific cellular response mediated by receptor trafficking. *J Cell Biol*. 2009:187:1101–1116.

Gage FH. Adult neurogenesis in mammals. *Science*. 2019:364(6443):827–828.

Ghosh HS. Adult neurogenesis and the promise of adult neural stem cells. *J Exp Neurosci*. 2019:13:1–12.

Gonçalves JT, Schafer ST, Gage FH. Adult neurogenesis in the hippocampus: from stem cells to behavior. *Cell*. 2016:167(4):897–914.

González-Billault C, Del Río JA, Ureña JM, Jiménez-Mateos EM, Barallobre MJ, Pascual M, Pujadas L, Simó S, La TA, Gavin R, et al. A role of MAP1B in Reelin-dependent neuronal migration. *Cereb Cortex*. 2005:15:1134–1145.

Hewitt CA, Ling KH, Merson TD, Simpson KM, Ritchie ME, King SL, Pritchard MA, Smyth GK, Thomas T, Scott HS, et al. Gene network disruptions and neurogenesis defects in the adult Ts1Cje mouse model of down syndrome. *PLoS One*. 2010:5:1–18.

Hussman JP, Chung RH, Griswold AJ, Jaworski JM, Salyakina D, Ma D, Konidari I, Whitehead PL, Vance JM, Martin ER, et al. A noise-reduction GWAS analysis implicates altered regulation of neurite outgrowth and guidance in autism. *Mol Autism*. 2011:2(1):1–16.

Jandial R, Singec I, Ames CP, Snyder EY. Genetic modification of neural stem cells. *Molecular therapy: the journal of the American Society of Gene Therapy*. 2008:16(3):450–457.

Kahlem P, Sultan M, Herwig R, Steinfath M, Balzereit D, Eppens B, Saran NG, Pletcher MT, South ST, Stetten G, et al. Transcript level alterations reflect gene dosage effects across multiple tissues in a mouse model of down syndrome. *Genome Res*. 2004:14(7): 1258–1267.

Karpowicz P, Willaime-Morawek S, Balenci L, Deveale B, Inoue T, Van Der Kooy D. E-cadherin regulates neural stem cell self-renewal. *J Neurosci*. 2009:29:3885–3896.

Kawauchi T, Hoshino M. Molecular pathways regulating cytoskeletal organization and morphological changes in migrating neurons. *Dev Neurosci*. 2008:30:36–46.

Kempermann G, Song H, Gage FH. Neurogenesis in the adult hippocampus. *Cold Spring Harbor perspectives in biology*. 2015:7(9): 1–14.

Kiselyov VV, Skladchikova G, Hinsby AM, Jensen PH, Kulahin N, Soroka V, Pedersen N, Tsetlin V, Poulsen FM, Berezin V, et al. Structural basis for a direct interaction between FGFR1 and NCAM and evidence for a regulatory role of ATP. *Structure*. 2003:11:691–701.

Kokovay E, Wang Y, Kusek G, Wurster R, Lederman P, Lowry N, Shen Q, Temple S. VCAM1 is essential to maintain the structure of the SVZ niche and acts as an environmental sensor to regulate SVZ lineage progression. *Cell Stem Cell*. 2012:11:220–230.

Kronenberg G, Gertz K, Baldinger T, Kirste I, Eckart S, Yildirim F, Ji S, Heuser I, Schröck H, Hörtnagl H, et al. Impact of actin filament stabilization on adult hippocampal and olfactory bulb neurogenesis. *J Neurosci*. 2010:30:3419–3431.

Kulahin N, Walmod PS. The neural cell adhesion molecule NCAM2/OCAM/RNCAM, a close relative to NCAM. *Adv Exp Med Biol*. 2010:663:403–420.

Kulahin N, Li S, Hinsby A, Kiselyov V, Berezin V, Bock E. Fibronectin type III (FN3) modules of the neuronal cell adhesion molecule L1 interact directly with the fibroblast growth factor (FGF) receptor. *Mol Cell Neurosci*. 2008:37:528–536.

Kumar A, Pareek V, Faiq MA, Ghosh SK, Kumari C. Adult neurogenesis in humans: a review of basic concepts, history, current research, and clinical implications. *Innov Clin Neurosci*. 2019:16: 30–37.

Kumar M., Keller B., Makalou N. & Sutton R. E. Systematic determination of the packaging limit of lentiviral vectors. *Human gene therapy*, 2001:12(15):1893–1905.

Leshchyns'Ka I, Liew H, Shepherd C, Halliday G, Stevens C, Ke YD, Ittner LM, Sytnyk V. Aβ-dependent reduction of NCAM2-mediated synaptic adhesion contributes to synapse loss in Alzheimer's disease. *Nat Commun*. 2015:6:1–18.

López-Hidalgo R, Ballestín R, Vega J, Blasco-Ibáñez JM, Crespo C, Gilabert-Juan J, Nácher J, Varea E. Hypocellularity in the murine model for down syndrome Ts65Dn is not affected by adult neurogenesis. *Front Neurosci*. 2016:10:1–13.

Lorenzi HA, Reeves RH. Hippocampal hypocellularity in the Ts65Dn mouse originates early in development. *Brain Res*. 2006:1104: 153–159.

Makino T, McLysaght A. Ohnologs in the human genome are dosage balanced and frequently associated with disease. *Proc Natl Acad Sci U S A*. 2010:107(20):9270–9274.

Marthiens V, Kazanis I, Moss L, Long K, Ffrench-Constant C. Adhesion molecules in the stem cell niche - more than just staying in shape. *J Cell Sci*. 2010:123(10):1613–1622.

Ming G, Song H. Adult neurogenesis in the mammalian brain: significant answers and significant questions. *Neuron*. 2011:70(4): 687–702.

Morante-Redolat JM, Porlan E. Neural stem cell regulation by adhesion molecules within the subependymal niche. *Front Cell Dev Biol*. 2019:7:1–8.

Morizur L, Chicheportiche A, Gauthier LR, Daynac M, Boussin FD, Mouthon MA. Distinct molecular signatures of quiescent and activated adult neural stem cells reveal specific interactions with their microenvironment. *Stem Cell Reports*. 2018:11:565–577.

Palmer CR, Liu CS, Romanow WJ, Lee MH, Chun J. Altered cell and RNA isoform diversity in aging down syndrome brains. *Proc Natl Acad Sci U S A*. 2021:118(47):1–11.

Parcerisas A, Pujadas L, Ortega-Gascó A, Perelló-Amorós B, Viais R, Hino K, Figueiro-Silva J, La Torre A, Trullás R, Simó S, et al. NCAM2 regulates dendritic and axonal differentiation through the cytoskeletal proteins MAP2 and 14-3-3. *Cereb Cortex*. 2020:30: 3781–3799.

Parcerisas A, Ortega-gascó A, Hernaiz-llorens M, Odena MA, Ulloa F, de Oliveira E, Bosch M, Pujadas L, Soriano E. New partners identified by mass spectrometry assay reveal functions of NCAM2 in neural cytoskeleton organization. *Int J Mol Sci*. 2021:22(14):1–20.

Parcerisas A, Ortega-Gascó A, Pujadas L, Soriano E. The hidden side of NCAM family: NCAM2, a key cytoskeleton organization molecule regulating multiple neural functions. *Int J Mol Sci*. 2021b:22:1–23.

Pébusque MJ, Coulier F, Birnbaum D, Pontarotti P. Ancient large-scale genome duplications: phylogenetic and linkage analyses shed light on chordate genome evolution. *Mol Biol Evol*. 1998:15: 1145–1159.

Petit F, Plessis G, Decamp M, Cuisset JM, Blyth M, Pendlebury M, Andrieux J. 21q21 deletion involving NCAM2: report of 3 cases with neurodevelopmental disorders. *Eur J Med Genet*. 2015:58: 44–46.

Porlan E, Martí-Prado B, Morante-Redolat JM, Consiglio A, Delgado AC, Kypta R, López-Otín C, Kirstein M, Fariñas I. MT5-MMP regulates adult neural stem cell functional quiescence through the cleavage of N-cadherin. *Nat Cell Biol*. 2014:16:629–638.

Rasmussen KK, Falkesgaard MH, Winther M, Roed NK, Quistgaard CL, Teisen MN, Edslev SM, Petersen DL, Aljubouri A, Christensen C, et al. NCAM2 fibronectin type-III domains form a rigid structure that binds and activates the fibroblast growth factor receptor. *Sci Rep*. 2018:8:1–13.

Scholz C, Steinemann D, Mälzer M, Roy M, Arslan-Kirchner M, Illig T, Schmidtke J, Stuhrmann M. NCAM2 deletion in a boy with macrocephaly and autism: cause, association or predisposition? *Eur J Med Genet*. 2016:59:493–498.

Seri B, García-Verdugo JM, Collado-Morente L, McEwen BS, Alvarez-Buylla A. Cell types, lineage, and architecture of the germinal zone in the adult dentate gyrus. *J Comp Neurol*. 2004:478:359–378.

Sheng L, Leshchyns'Ka I, Sytnyk V. Neural cell adhesion molecule 2 promotes the formation of filopodia and neurite branching by inducing submembrane increases in Ca2+ levels. *J Neurosci*. 2015:35:1739–1752.

Shin J, Berg DA, Zhu Y, Shin JY, Song J, Bonaguidi MA, Enikolopov G, Nauen DW, Christian KM, Ming GL, et al. Single-cell RNA-Seq with waterfall reveals molecular cascades underlying adult neurogenesis. *Cell Stem Cell*. 2015:17:360–372.

Simó S, Jossin Y, Cooper JA. Cullin 5 regulates cortical layering by modulating the speed and duration of DAB1-dependent neuronal migration. *J Neurosci*. 2010:30:5668–5676.

Sweeney N. P. & Vink C. A. The impact of lentiviral vector genome size and producer cell genomic to gag-pol mRNA ratios on packaging efficiency and titre. Molecular therapy. *Methods & Clinical Development*. 2021:21:574–584.

Teixeira CM, Kron MM, Masachs N, Zhang H, Lagace DC, Martinez A, Reillo I, Duan X, Bosch C, Pujadas L, et al. Cell-autonomous inactivation of the reelin pathway impairs adult neurogenesis in the hippocampus. *J Neurosci*. 2012:32:12051–12065.

Urbán N, Guillemot F. Neurogenesis in the embryonic and adult brain: same regulators, different roles. *Front Cell Neurosci*. 2014:8:1–19.

Urbán N, Blomfield IM, Guillemot F. Quiescence of adult mammalian neural stem cells: a highly regulated rest. *Neuron*. 2019:104(5): 834–848.

Von Campenhausen H, Yoshihara Y, Mori K. OCAM reveals segregated mitral/tufted cell pathways in developing accessory olfactory bulb. *Neuroreport*. 1997:8:2607–2612.

Walker TL, Kempermann G. One mouse, two cultures: isolation and culture of adult neural stem cells from the two neurogenic zones of individual mice. *Journal of visualized experiments: JoVE*. 2014:84:1–9.

Winther M, Berezin V, Walmod PS. NCAM2/OCAM/RNCAM: cell adhesion molecule with a role in neuronal compartmentalization. *Int J Biochem Cell Biol*. 2012:44(3):441–446.

Xie XP, Laks DR, Sun D, Poran A, Laughney AM, Wang Z, Sam J, Belenguer G, Fariñas I, Elemento O, et al. High-resolution mouse subventricular zone stem-cell niche transcriptome reveals features of lineage, anatomy, and aging. *Proc Natl Acad Sci U S A*. 2020:117:31448–31458.

Yao B, Christian KM, He C, Jin P, Ming GL, Song H. Epigenetic mechanisms in neurogenesis. *Nat Rev Neurosci*. 2016:17(9): 537–549.

Zhang L, Zhang X. Factors regulating neurogenesis in the adult dentate gyrus. In Stuchlik A, editor. *The hippocampus – plasticity and functions*. London: InTech; 2018. p. 17–48.

Zhao C, Deng W, Gage FH. Mechanisms and functional implications of adult neurogenesis. *Cell*. 2008:132(4):645–660.